European Journal of Medicinal Chemistry 306 (2026) 118621

Contents lists available at ScienceDirect

European Journal of Medicinal Chemistry

journal homepage: www.elsevier.com/locate/ejmech

Research paper

New fluoxetine analogues as anti-enterovirus agents targeting 2C protein

Safeh Khemiri [a,1], Marine O. Faucher [b,1], Stephane Bourg [c], Sarah Attoumani-Madi [b], Carole Yaacoub [b], Franck Touret [b], Marc Farag [c], Mattéo Fermiana Vitorino [a], Pascal Bonnet [c], Patrice Vanelle [a], Samia Aci-Seche [c], Bruno Coutard [b,*,1], Karine Barral [a,**,1]

[a] Aix Marseille Univ, CNRS, ICR, Marseille, France
[b] Unité des Virus Émergents (UVE: Aix-Marseille Univ, Università di Corsica, IRD 190, Inserm 1207, IRBA), France
[c] Université D'Orléans, CNRS, ICOA, UMR7311, Orléans, France

ARTICLE INFO

Keywords:
Enterovirus
2C protein
Fluoxetine derivatives
Broad-spectrum inhibitor
antiviral

ABSTRACT

There are currently no antiviral drugs available to treat or prevent life-threatening human non-poliovirus enterovirus infections, such as those caused by CV-B3, EV-A71 or EV-D68. Our aim is to develop novel inhibitors that target the non-structural ATPase/Helicase 2C protein, which is involved in the RNA replication process that is essential for enterovirus replication, among other functions. In this study, we describe the optimization of (*S*)-fluoxetine, a promising hit identified through drug repurposing that binds to an allosteric site on the CV-B3 2C ATPase domain. Our optimization process was guided by rational design, X-ray crystallographic structures, computational docking, and validation by enzyme and cell-based assays, leading to several new inhibitors, among which compound **53** (CV–B3 EC_{50} = 0.5 μM and EV-D68 EC_{50} = 0.4 μM), a novel anti-enterovirus with higher selectivity indexes than (*S*)-fluoxetine.

1. Introduction

Enteroviruses, belonging to the *Picornaviridae* family, are among the most prevalent viruses infecting humans worldwide, making them a growing public health concern [1]. To date, there are four enterovirus (EV) species (EV-A to EV-D) and three rhinovirus species (RV-A to RV-C) infecting humans. These species include, among others, polioviruses (PV; EV-C), which cause poliomyelitis, coxsackieviruses (CV-A, CV-B; EV-A to EV-C), and echoviruses (E; EV-B). Infections with enteroviruses can cause a wide range of diseases, from the common cold to hand-foot-and-mouth disease (HFMD), meningitis, myocarditis, encephalitis, and acute flaccid paralysis [2–4]. Although these viral infections are often self-limiting, they can also result in serious complications, especially in young children and immunocompromised patients.

Enteroviruses continue to pose a significant public health challenge, with new strains emerging and others persisting despite vaccination efforts. The recent emergence of EV-A71 in South-East Asia and EV-D68 in North America, both associated with severe neurological complications, has underscored the ongoing threat these viruses present [5,6]. While the global campaign against poliovirus has greatly reduced its prevalence, recent cases demonstrate that complete eradication remains elusive [7]. Although an inactivated EV-A71 vaccine has been approved in China and shown to be effective, the co-circulation of numerous enterovirus serotypes and their rapid genetic evolution make single-virus vaccine strategies inadequate [8]. With over 100 enteroviruses (EVs) and more than 150 rhinoviruses (RVs) identified, developing a universal vaccine is unlikely, highlighting the urgent need for broad-spectrum antiviral therapies.

A promising therapeutic approach is to develop direct-acting antivirals (DAAs) that target viral proteins. These include the 2C protein, which is highly conserved among enteroviruses and plays a key role in several stages of the virus life cycle, making it an attractive target for the development of broad-spectrum treatments. Structural and functional studies have highlighted the various biological functions of the 2C protein in the viral cycle, in particular its involvement in the viral replication complex and ATPase activity [9–14].

Several Food and Drug Administration (FDA)-approved compounds have been identified by drug repositioning as inhibitors of the 2C protein, including fluoxetine (Fig. 1), dibucaine, pirlindole, and

* Corresponding author.
** Corresponding author.
E-mail addresses: bruno.coutard@univ-amu.fr (B. Coutard), karine.barral@univ-amu.fr (K. Barral).
[1] These authors contributed equally.

https://doi.org/10.1016/j.ejmech.2026.118621
Received 14 November 2025; Received in revised form 20 January 2026; Accepted 23 January 2026
Available online 28 January 2026

zuclopenthixol [15–18]. One of the most extensively studied is fluoxetine (Prozac®), a selective serotonin reuptake inhibitor (SSRI), that is approved for the treatment of depression and anxiety disorders. The *in vitro* anti-enterovirus activity of fluoxetine was first demonstrated in 2012 by Zuo et al. [15]. A second study has shown that fluoxetine interferes with viral RNA replication by binding to the 2C protein, and selectively inhibits replication of EV-B (EC_{50} CV-B3 = 3.36 μM) and EV-D (EC_{50} EV-D68 = 1.35 μM) [16]. In 2019, Bauer et al. demonstrated through mechanistic studies that (*S*)-fluoxetine directly binds (Kd = 9.5 μM) with higher affinity than (*R*)-fluoxetine (Kd > 200 μM). This stereospecificity also applies to inhibition of the replication of EV-D68. However, neither the racemic mixture nor (*S*)-fluoxetine were active against EV-A71 and PV-1 in infected cells, at concentrations where (*S*)-fluoxetine is not toxic *in vitro* [19]. In addition, the crystallographic structure of CV-B3 protein 2C in complex with (*S*)-fluoxetine (PDB IDs 6S3A and 6T3W) revealed that (*S*)-fluoxetine binds to an allosteric site in the ATPase domain of CV-B3 2C protein. A more detailed biochemical study, together with cryo-electron microscopy analysis, elucidated the mechanism of action (*S*)-fluoxetine, which its binding locks the hexameric structure of protein 2C, inhibiting its ATPase activity [13].

Although (*S*)-fluoxetine inhibits viral replication of EV-B and EV-D *in vitro*, its effective dose (EC_{50} CV-B3∼1 μM) is close to its cytotoxic dose ($CC_{50} \approx 25$ μM), so its therapeutic window as an antiviral treatment is quite narrow, and (*S*)-fluoxetine has shown no significant antiviral efficacy *in vivo* in EV-D68 infected mouse models [20]. However, fluoxetine may have been effective in treating severe cases of chronic infections (enterovirus encephalitis and meningoencephalitis) [21,22]. At this point, (*S*)-fluoxetine can be considered a promising 'hit' paving the way for an optimization process. Previous work reported the evaluation of six different fragments derived from fluoxetine to identify its key moieties involved in targeting 2C CB-V3 [19]. Only the *N*-methyl-3-[4-(trifluoromethyl)phenoxy]propan-1-amine fragment exhibited modest antiviral activity indicating that *para*-(trifluoromethyl)phenoxy and N-methylamine moieties are the ones involved in the antiviral effect, whereas the non-substituted phenyl ring seems dispensable. Here, we report a structure-activity relationships (SAR) study mainly focused on structural modifications of the *para*-(trifluoromethyl)phenoxy (series 3, Fig. 1) and N-methylamine moieties of fluoxetine (series 1, Fig. 1) to potentially improve its antiviral efficacy, reduce toxicity and broaden its spectrum of action among enteroviruses.

2. Results and discussion

2.1. Rational design and synthesis of (S)-fluoxetine analogues from series 1, 2, 3 & 4

A first rational design was performed to investigate structural modifications around four distinct series of (*S*)-fluoxetine analogues described in Fig. 1. For series 1, the N-methylamine moiety was replaced by various aliphatic, carbocyclic and heterocyclic amines starting from a simple *N,N*-dimethylamine to bulkier phenyl- and benzylpiperazine groups. For series 2 and 4, we explored a single modification by replacing the non-substituted phenyl ring by a thiophene (series 2) and the phenoxy by a thiophenoxy moiety (series 4), respectively. The last moiety of interest was *para*-(trifluoromethyl)phenoxy (series 3) and we started replacing the *para*-trifluoromethyl group by known (bio)isosteres such as halogen atoms and electronically close groups with similar size or shape (CH_3O-, CF_3O-, CH_3-, CN-, CF_3SO_2-). We also replaced the *para*-trifluoromethyl group by a phenyl and a benzyl to explore potential *π-stacking interactions*. Regarding the reported data by Manganaro et al. [23], we prioritized all these modifications in *para* position since changing the CF_3 substituent from *para* to *ortho* or *meta* position abolished the antiviral activity.

The synthesis of analogues from series 1 started the conversion of commercial (*S*)-3-chloro-1-phenyl-1-propanol to (*S*)-3-iodo-1-phenyl-1-propanol **2** using NaI with acetone via a Finkelstein reaction [24] in 93 % yield (Scheme 1). Reactions with iodopropanol **2** with excess of

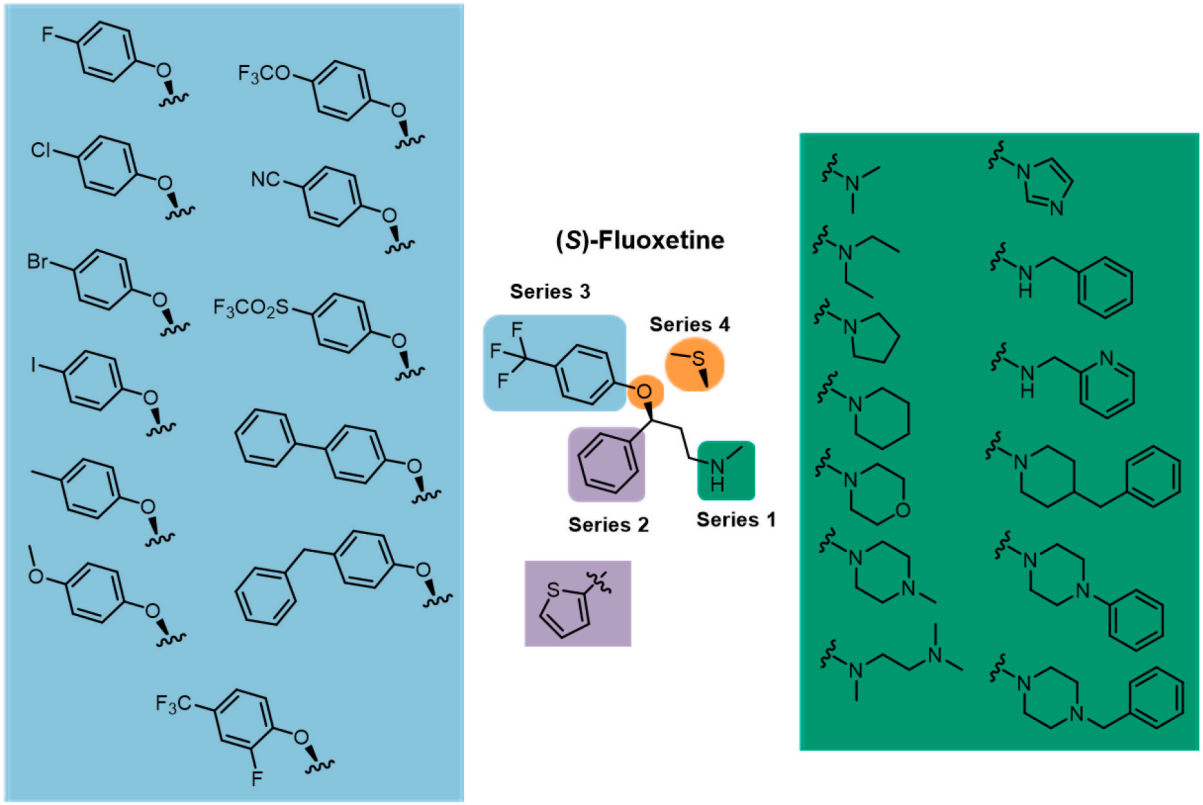

Fig. 1. Rational design and structural modifications around four distinct series of (*S*)-fluoxetine analogues.

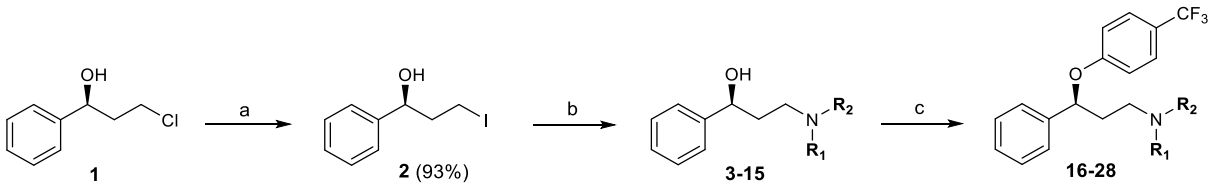

Reagents and conditions: (a) NaI, acetone, reflux, 48h; (b) amine derivative, dry THF, rt, 3-24h; (c) 4-chlorobenzotrifluoride, NaH, dry DMF, 100°C, 4h.

Compounds		Yield (%)	Compounds		Yield (%)
3 **16**		36 17	**10** **23**		83 43
4 **17**		48 34	**11** **24**	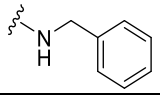	68 27
5 **18**	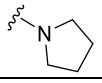	65 75	**12** **25**	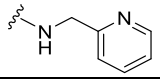	73 13
6 **19**		54 13	**13** **26**	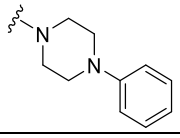	85 20
7 **20**	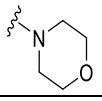	59 39	**14** **27**	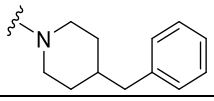	90 18
8 **21**	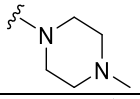	60 17	**15** **28**	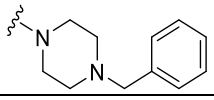	27 35
9 **22**	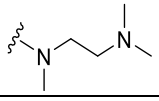	47 26			

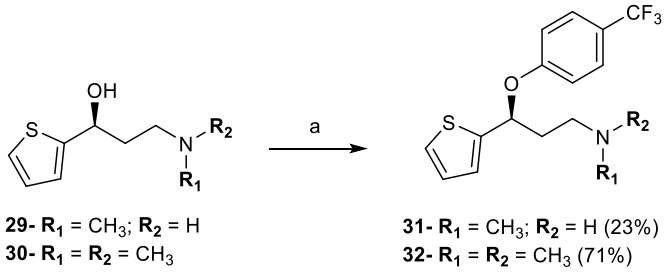

Reagents and conditions: (a) 4-chlorobenzotrifluoride, NaH, dry DMF, 100°C, 2-5h.

Scheme 1. Synthesis of analogues **16–28** (series 1) and analogues **31–32** (series 2) via a SNAr reaction.

selected amines in dry THF gave the corresponding derivatives **3–15** with moderate to good yields. Then, the desired analogues **16–28** were obtained by a nucleophilic aromatic substitution (SNAr) of 4-chlorobenzotrifluoride with alkoxide anions of derivatives **3–15** generated by reacting with NaH in dry DMF at 100 °C [25].

To confirm retention of the (*S*)-configuration of the chiral center core during the SNAr step, we performed a chiral analytical HPLC analysis on compound **16** (see experimental section and Fig. 1). There is no significant decrease of its enantiomeric excess in relation to the starting material used (ee values of 93 % for **16** versus 95 % for starting material).

In a same manner, we synthetized two analogues from series 2, starting with commercial (*S*)-3-(methylamino)-1-(2-thienyl)-1-propanol **29** and (*S*)-3-(dimethylamino)-1-(2-thienyl)-1-propanol **30** (Scheme 1) and giving compounds **31** and **32** with 23 % and 71 % yields respectively.

Regarding the synthesis of analogues from series 3, we employed an alternative synthetic pathway using a Mitsunobu reaction. Indeed, the previously described SNAr reaction is not appropriate for synthetizing *para-halogenated phenoxy derivatives and the use of commercial para-substituted phenols as reactants offers more substitution options.* For this purpose, we started to protect the secondary amine group of the commercial methyl (*R*)-3-(methylamino)-1-phenylpropan-1-ol **33** with di-*tert*-butyl dicarbonate in dry DCM, leading to the intermediate **34** in 98 % yield (Scheme 2) [23]. A Mitsunobu reaction between intermediate

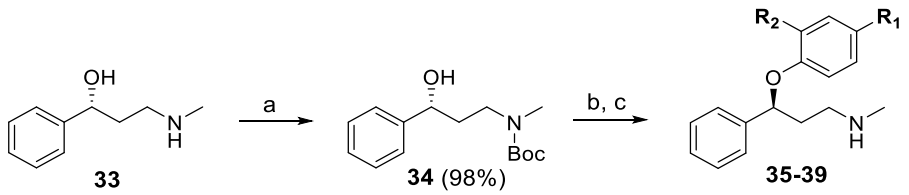

Reagents and conditions: (a) Boc_2O, dry DCM, rt, 24h; (b) phenol derivative, PPh_3, DIAD, dry THF, rt, 4-18h, (c) TFA, DCM, rt, 2-7h.

Compounds	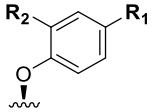	Yield (%)	Compounds	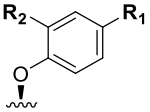	Yield (%)
35	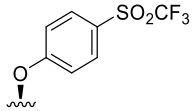	10	**38**	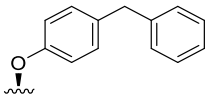	8
36	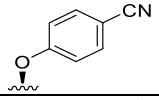	25	**39**	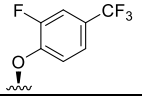	24
37	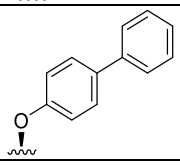	22			

Scheme 2. Synthesis of analogues **35–39** (series 3) via a Mitsunobu reaction.

34 and 1 equivalent of selected substituted phenols in the presence of diisopropyl azodicarboxylate (DIAD) and triphenylphosphine [26] gave the expected *para*-substituted (*S*)-fluoxetine analogues but despite several attempts to purify them by flash chromatography on silica gel, they could not be isolated from unreacted phenol. Therefore, we carried out the deprotection of the crude Boc-protected amine derivatives (in mixture with corresponding phenol) using TFA in DCM [23] to isolate the desired analogues **35–39** with moderate to low overall yields.

To overcome these limitations, we performed a similar Mitsunobu reaction between the commercial (*R*)-3-chloro-1-phenylpropan-1-ol **40** and other selected *para*-substituted phenols [26] (Scheme 3) and we obtained analogues **41–49** with slightly better yields and no purification issue. Then, analogues **41–49** reacted with **an** excess of aqueous methylamine (40 %) in ethanol at 120 °C in a sealed tube [27] leading to the desired *para*-substituted (*S*)-fluoxetine analogues **50–58** with moderate yields.

For series 4, a similar coupling with Mitsunobu reaction between (*R*)-3-chloro-1-phenylpropan-1-ol **40** and 4-(trifluoromethyl)thiophenol followed by a methylamination reaction, led to (*S*)-fluoxetine analogue **60** in which the phenoxy was replaced by a thiophenoxy moiety (Scheme 3).

To validate the Mitsunobu inversion and (*S*)-configuration of the chiral center core for the synthetized analogues, we performed a chiral analytical HPLC analysis on compound **53** (see experimental section and Fig. 2). No detectable racemisation occurred in the Mitsunobu reaction, and an enantiomeric excess of 99 % was obtained.

2.2. *In silico design and synthesis of (S)-fluoxetine analogues from series 3*

In a second stage, we extended our hit-to-lead optimization by employing a structure-based drug design (SBDD) approach using the crystal structure of (*S*)-fluoxetine complexed with CV-B3 2C protein available on the PDB (PDB IDs 6S3A). Based on the two main synthetic pathways previously described to synthetize (*S*)-fluoxetine analogues, we aimed to dock a library of virtual analogues designed from substituted chloro- or fluorobenzene (SNAr reaction) or phenol (Mitsunobu reaction) derivatives available in our laboratory. A first dataset of 140 compounds was designed and docked into the CV-B3 2C protein allosteric binding site (see experimental section and additional file in Supporting Information).

Two docking protocols were evaluated using Glide software. The (*S*)-fluoxetine was docked and ranked in the allosteric site by using standard precision (SP) and extra precision (XP) scoring functions with default settings. Docking results were then assessed with RMSD (root mean square deviation) of each predicted pose versus the crystal structure. Using these two scoring functions, we obtained a low RMSD value for the best pose between the docked (*S*)-fluoxetine and the crystallographic conformation (RMSD = 0.68 Å and RMSD = 0.65 Å for SP and XP scoring function respectively), with a better score for XP ($SP_{score} = -8.35$ and $XP_{score} = -9.17$). Therefore, all the following docking experiments are performed with extra precision (XP).

We then performed the docking of the 140 molecules (corresponding to 163 3D structures including tautomers and stereoisomers, see experimental section) using only XP score. Among the twenty ten top-score compounds, we selected ten molecules for synthesis (Table 1).

The predicted binding mode of **VS01**, the best scored molecule, is almost identical to the crystallographic structure of (*S*)-fluoxetine with a RMSD value of 0.4 Å between the two conformations (Fig. 2). The binding is mainly driven by hydrophobic interactions between the two aromatic rings of the compounds and the residues of two hydrophobic pockets composed of L157, P159, M175, D176 for one pocket and L178, P182, V187, F190, L238, F242 for the other one. Moreover, **VS01**, as (*S*)-fluoxetine, is engaged in two hydrogen bonds with the protein. The first one is formed with the backbone and the side chain of C179 and involves the oxygen atom of the ether moiety whereas the second one occurs between the methylamine group of the compounds and the side chain of D186.

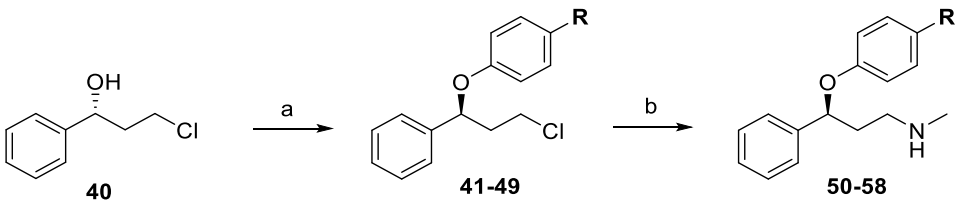

Reagents and conditions: (a) phenol derivative, PPh_3, DIAD, dry THF, rt, 3-16h,
(b) 40% aq. methylamine, EtOH, 120°C, 1h.

Compounds	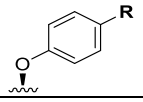	Yield (%)	Compounds	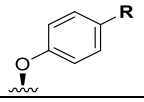	Yield (%)
41 **50**	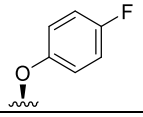	27 62	**46** **55**	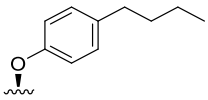	34 24
42 **51**	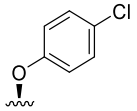	35 58	**47** **56**	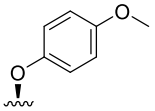	18 21
43 **52**	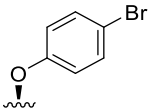	65 46	**48** **57**	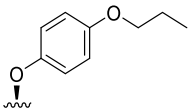	18 16
44 **53**	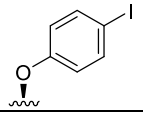	33 59	**49** **58**	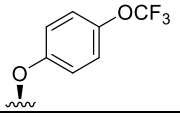	44 76
45 **54**	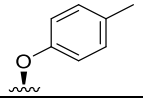	70 43			

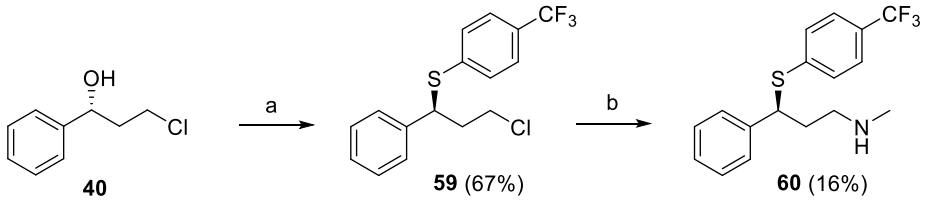

Reagents and conditions: (a) 4-(trifluoromethyl)thiophenol, PPh_3, DIAD, dry THF, rt, 30h,
(b) 40% aq. methylamine, EtOH, 120°C, 1h.

Scheme 3. Synthesis of analogues **50–58** (series 3) and **60** (series 4) via a Mitsunobu reaction followed by a methylamination reaction.

The synthesis of analogues from **VS01, VS04** and **VS09** was achieved by a one-step SNAr of chlorobenzene derivatives with commercial (*S*)-3-(methylamino)-1-phenylpropan-1-ol **61** using the same protocol with NaH in dry DMF at 100 °C (Scheme 4). The trifluoromethylpyridine analogue **62** was obtained from **VS01** with 27 % yield. Despite several attempts in different reaction conditions, commercial (*S*)-3-(methylamino)-1-phenylpropan-1-ol **61** failed to react with chlorobenzene derivatives **VS04** and **VS09**. This lack of reactivity is probably due to the lack of strongly electron-attracting groups located on the aryl halide rings at *ortho-para* positions, that stabilize the anionic intermediate formed.

For synthesis of analogues from **VS02–03, VS05–08, VS10** we performed a Mitsunobu reaction between the commercial (R)-3-chloro-1-phenylpropan-1-ol **40** and selected phenols (Scheme 4). For **VS06–07** and **VS10** derivatives, containing an aminophenol group, direct substitutions were attempted but gave very low yields. So, we attempted these Mitsunobu substitutions using the corresponding nitrophenol derivatives. We obtained analogues **63–69** with low to moderate yields, that reacted with an excess of aqueous methylamine (40 %) in ethanol leading to the final (*S*)-fluoxetine analogues **70–73** and the nitrobenzene intermediates **74–76**. Then, the aryl nitro group of **74–76** was reduced to the desired aniline with stannous chloride in ethyl acetate at 70 °C yielded the final derivatives **77–79** [28,29].

2.2.1. Antiviral evaluation of synthetized compounds on CV-B3, EV-A71 and EV-D68 in infected cells

The synthetized compounds **16–28**, **31–32**, **35–39**, **50–58**, **60**, **62** and **70–79** were initially evaluated for their potential inhibitory effect on CV-B3 *in vitro* replication in HeLa CCL-2 cells (Table 2, Fig. 3A, Fig. S3), using a virus yield inhibition assay as previously described.30 (*S*) and (*R*)-fluoxetine were used as positive and negative controls, respectively. Seproxetine, the (*S*)-enantiomer of Norfluoxetine, the

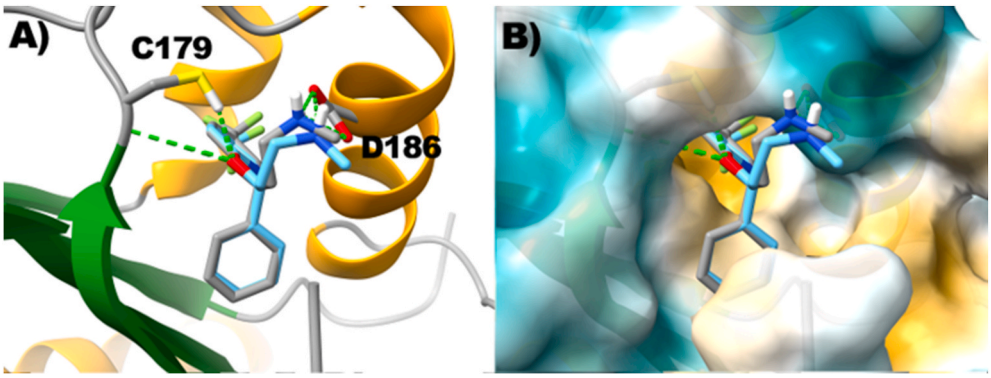

Fig. 2. 3D representation of the docking poses of **VS01**, represented as cyan sticks, compared to the crystallographic pose of (*S*)-fluoxetine, represented as grey sticks. Hydrogen bonds are highlighted with green dotted lines. A) The protein structure is represented as a ribbon with helices in orange, strands in green and coils in grey. B) The protein structure is represented using both ribbon and surface (transparent rendering) colored from orange for hydrophobic areas to cyan for hydrophilic areas.

Table 1
2D structure of compounds selected by virtual screening (VS). The building blocks used to build the compounds are depicted with reactive groups highlighted in red.

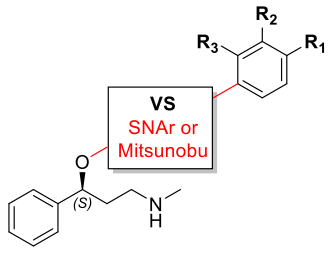

VS ID	Substructure	Glide score (kJ/mol)	VS ID	Substructure	Glide score (kJ/mol)
VS01	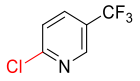	−9.79	**VS06**	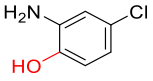	−8.51
VS02	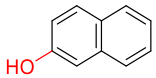	−9.17	**VS07**	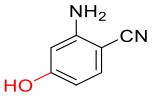	−8.38
VS03	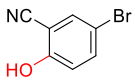	−8.85	**VS08**	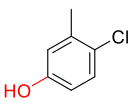	−8.15
VS04	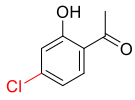	−8.79	**VS09**	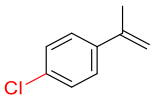	−8.05
VS05	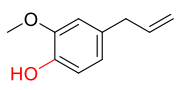	−8.79	**VS10**	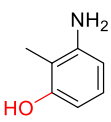	−7.94

N-demethylated main metabolite of fluoxetine acting as a selective serotonin inhibitor was also included in the experimental setting.

To calculate these parameters, a non-linear regression was performed as described in the Methods section, using triplicates for each compound. For compounds with an SI > 15, the corresponding error bars (mean ± standard deviation) are shown on the curves in Fig. 3 and S3.

Initially, considering the selectivity index (SI) for compound selection, the most promising inhibitors against CV-B3 (SI > 15), namely compounds **16**, **18**, **22**, **31**, **53** and seproxetine, were tested against EV-A71 and EV-D68 to evaluate their antiviral spectrum *in vitro*. Vapendavir and A-967079, previously described as inhibitors of EV-A71 and EV-D68 respectively, were used as positive controls in these assays (Fig. 3B and C, Table 3, Figs. S4 and S5) [31,32]. To confirm that the inhibition of viral replication, as evidenced by a reduction in viral RNA copy number, correlates with a decrease in the number of infected cells, a plaque assay and a cytopathic effect (CPE) assay were conducted using compound **53** against EV-D68 (Fig. 3D and E). Visual inspection of the plaque assay and determination of the CPE-based EC50 both confirm a correlation between molecular titer and viral infection.

Like fluoxetine, all of the tested compounds were efficient to inhibit EV-D68 replication. In particular, compounds **16** and **31** have a potency against EV-D68 replication comparable to that of (*S*)-fluoxetine, and are twice as less cytotoxic than (*S*)-fluoxetine, which increases their selective index higher than or close to 100, respectively.

Compounds **16**, **18**, **22** and **31** did not inhibit EV-A71. For compound **53**, seproxetine and (*S*)-fluoxetine, the measured EC_{50} are close to their CC_{50} (e.g., EC_{50} (**53**) = 8 μM, CC_{50} (**53**) = 23 μM), making it difficult to determine whether the observed inhibition is due to a gain in antiviral effect or a result of the cytoxicity effect (Fig. 3C).

To calculate these parameters, a non-linear regression was performed as described in the Methods section, using triplicates for each compound. The corresponding error bars (mean ± standard deviation) are shown on the curves in Fig. 3, S4 and S5.

For series 1, there is no clear influence of the substituents. It may be due to the fact that this substituent is exposed to the solvent area, as shown in Fig. 2. This could explain the loss of activity for compounds **26**, **27**, and **28**, exposing a large hydrophobic group to the solvent area.

Regarding series 3, the 4-(trifluoromethyl)phenyl moiety of (*S*)-fluoxetine is located in a small hydrophobic pocket (Fig. 2). That may explain that the substitution of trifluoromethyl group by a halogen atom mimicking hydrophobic interactions maintains the activity of the compound. We clearly observed an improvement in activity when increasing the size of the halogen atom I (**53**) > Br (**52**) > Cl (**51**) > F (**50**). However, adding polar atoms (compounds **56**, **57** and **58**) or large substituents on the *para* substitution of the phenyl, even hydrophobic, as for compounds **37** and **38**, decreases activity compared to (*S*)-fluoxetine.

*2.2.2. Evaluation of the binding of compounds **16**, **18**, **22**, **31**, **53**, seproxetine and (S)-fluoxetine to CV-B3 and EV-A71 2C proteins*

The binding capacity of compounds **16**, **18**, **22**, **31**, **53** and seproxetine to the Δ36-2C protein (lacking the 36 N-terminal residues) of CV-

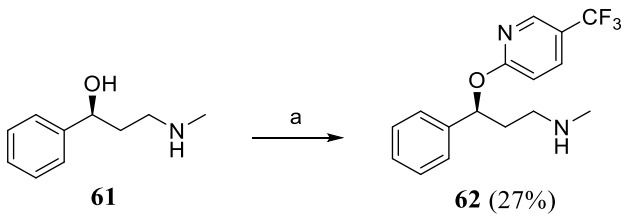

Reagents and conditions: (a) 2-chloro-5-(trifluoromethyl)pyridine, NaH, dry DMF, 100°C, 5h.

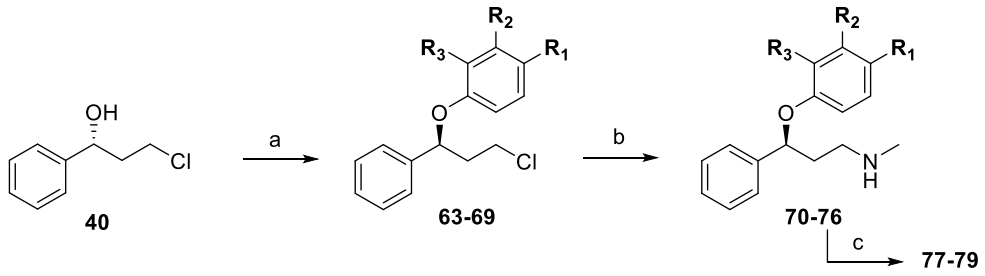

Reagents and conditions: (a) phenol derivative, PPh_3, DIAD, dry THF, rt, 3-16h, (b) 40% aq. methylamine, EtOH, 120°C, 1h; (c) $SnCl_2$, EtOAc, 70°C, 2h.

Compounds	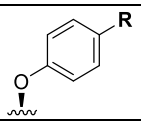	Yield (%)	Compounds	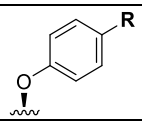	Yield (%)
63 **70**	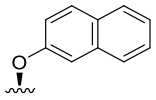	34 65	**68** **75**	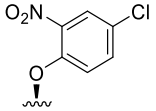	45 20
64 **71**	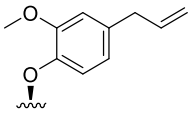	17 16	**69** **76**	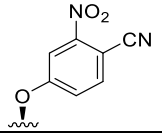	84 23
65 **72**	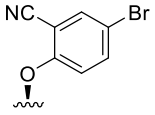	44 38	**77**	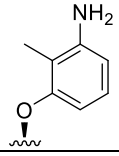	22
66 **73**	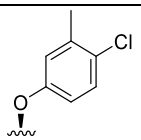	20 70	**78**	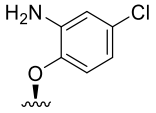	35
67 **74**	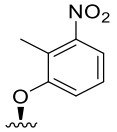	42 40	**79**	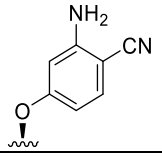	5

Scheme 4. Synthesis of analogues **62** via a SNAr reaction and analogues **70–79** via a Mitsunobu reaction.

B3 was evaluated by Thermal Shift Assay (TSA), as previously described [19]. In this assay, an increase of the melting temperature (T_m) reflects a stabilization of the protein, as a result of a stabilizing interaction between the protein and the compound. Like (*S*)-fluoxetine, compounds **16**, **31**, **53** and seproxetine induced an inhibitor concentration-dependent increase in the T_m of 2C protein, indicating an interaction between these compounds and the 2C, with a possible Mode of Action comparable to that of (*S*)-fluoxetine (Fig. 4, Fig. S6). Compounds **18** and **22** induced a $\Delta T_m < 0.5$ °C, suggesting a weaker interaction energy compared to (*S*)-fluoxetine.

We also assessed the binding capacity of (*S*)-fluoxetine, compound **53**, and seproxetine to the Δ116-2C protein of EV-A71 (Fig. 5, Fig. S7). Guanidine hydrochloride (HCl) was used as a positive control, since its anti-EV-A71 activity has been previously reported at mM range [10]. At a final concentration of 1 mM, Guanidine HCl induced a 0.6 °C increase in the 2C T_m, indicating an interaction with the protein. At a final

Table 2
In vitro antiviral activity and cytotoxicity of compounds **16–28**, **31–32**, **35–39**, **50–58**, **60**, **62**, **70–79,** seproxetine, (*S*)- and (*R*)-fluoxetine against CV-B3 in HeLa CCL-2 cells.

Compounds	EC_{50} (μM) CV-B3	CC_{50} (μM) HeLa CCL-2	SI	Compounds	EC_{50} (μM) CV-B3	CC_{50} (μM) HeLa CCL-2	SI
16	2.9	43	15	**50**	–	32	–
17	3.8	45	12	**51**	4.5	33	7
18	1.4	32	23	**52**	3.6	40	11
19	3.0	30	10	**53**	0.5	22	44
20	> 8	37	<5	**54**	3.3	32	10
21	> 8	47	<6	**55**	–	17	–
22	1.2	24	20	**56**	–	> 100	–
23	2.2	25	11	**57**	–	47	–
24	3.4	12	4	**58**	> 8	24	<3
25	2.4	15	6	**60**	–	12	–
26	> 8	12	<2	**62**	–	32	–
27	–	14	–	**70**	–	22	–
28	–	15	–	**71**	–	46	–
31	1.7	27	16	**72**	3.5	22	6
32	> 8	48	<6	**73**	3.7	17	5
35	–	29	–	**74**	> 8	47	<6
36	> 8	100	<12.5	**75**	–	83	–
37	–	17	–	**76**	–	24	–
38	2.5	24	9.6	**77**	–	> 100	–
39	–	24	–	**78**	–	50	–
(*S*)-Fluoxetine	0.8	24	30	**79**	–	> 100	–
(*R*)-Fluoxetine	–	23	–	**Seproxetine**	0.9	22	24

SI: selectivity index (CC_{50}/EC_{50}); (−): no antiviral effect in the tested concentration range.

inhibitor concentration of 500 μM, (*S*)-fluoxetine, compound **53**, and seproxetine induced a decrease in the T_m of EV-A71 2C protein ≥1.5 °C, which is indicating protein destabilization, indicative of possible specific or non-specific binding at high concentrations.

Given that compounds **16**, **18**, **53**, and seproxetine binds to the CV-B3 2C protein, we assessed their ability to inhibit 2C ATPase activity. Since the ATPase activity of 2C is dependent on its hexameric conformation, we used for this assay a recombinant protein in which the 116 N-terminal residues are replaced by a soluble MBP-hexamerization domain, hereafter named MBP-Hex-2CΔ116, as previously described [13]. In our assay, compounds **53** and seproxetine efficiently inhibited the ATPase activity of the CV-B3 MBP-Hex-2CΔ116, with an IC_{50} comparable to that to (*S*)-fluoxetine (Fig. 5A). With compounds **16** and **18**, we were unable to measure any inhibition of the enzyme activity, that may be due to an inability of the compounds to inhibit the 2C ATPase activity *in vitro*, or to an incompatibility of the compounds with this assay.

2.3. X-ray crystallographic structure of CV-B3 2C protein in complex with compound *53*

To validate the binding mode of one of the most potent inhibitors, we co-crystallized the truncated CV-B3 Δ116-2C protein, used to obtain the crystal structure in complex with (*S*)-fluoxetine (PDB IDs 6S3A and 6T3W) [13] in the presence of compound **53**. We identified a crystallization condition that yielded crystals suitable for structure determination at 1.7 Å resolution, with a reliable electron density corresponding to compound **53** (PDB ID 9RQK), confirming a shared binding mode to (*S*)-fluoxetine (Fig. 6) in the expected allosteric binding site.

Electron density maps of (*S*)-fluoxetine and compound **53** overlap in crystal structures, indicating a similar binding mode. The binding mode of compound **53** on 2C protein is mainly promoted by hydrophobic interactions involving the residues L157, P158, P159, M175, D176, L178, C179, P182, D186, V187, F190 and L238, as it is the case for (*S*)-fluoxetine (Fig. 6).

Secondarily, hydrogen bonds between the methylamine group of (*S*)-fluoxetine with the backbone carbonyl of P159 and carboxylic acid side chain of D186 remain in complex with compound **53**, although weaker (~4.0 Å vs ~ 3.0 Å for (*S*)-fluoxetine).

2.4. Optimization by combining efficient structural modifications from series 1 and 3

We expected that by combining the structural modifications of the most potent and less cytotoxic inhibitors synthesized from series 1 and 3, we would obtain even more effective inhibitors while maintaining the original binding mode. Analogues **16** (dimethylamine moiety) and **18** (pyrrolidone moiety) were selected for series 1 and analogue **53** (*para*-iodophenoxy moiety) was selected for series 3, respectively. The previous synthetic pathways were combined and two new compounds **81–82** were synthesized and evaluated (Scheme 5, Table 4). For this purpose, we performed the same previous Mitsunobu protocol between (*R*)-3-chloro-1-phenylpropan-1-ol **40** and 4-iodophenol to obtain intermediate **80** with 43 % yield, which was converted by a one-pot, two-steps substitution using NaI [24] and excess of selected amines in dry THF to give the corresponding derivatives **81–82**.

We also combined the most potent structural modification from series 3, i.e. analogue **53** with its *para*-iodophenoxy moiety, with the most potent structural modification of the methylamine group (series 1) reported in Manganaro et al. [23], which is substituted by guanidine moiety. To do so, we performed a Gabriel reaction to convert compound **80** into the corresponding phtalimide derivative through a nucleophilic substitution, followed directly by a hydrazinolysis reaction using hydrazine monohydrate in ethanol to obtain the primary amine derivative **83** with 68 % yield. The derivative **83** was converted to the final derivative **84** with an excellent yield using the attractive guanidinylation reagent 1*H*-pyrazole-1-carboxamidine hydrochloride [33,34].

Since compounds **81** to **84** are derived from inhibitors effective against CV-B3 and EV-D68, we assessed their antiviral effect against these two viruses *in vitro* (Table 4).

None of these compounds, combining two structural modifications, demonstrated improved selectivity index against CV-B3, as compared to (*S*)-fluoxetine and compound **53**. Surprisingly, compound **81** did not show any inhibition against CV-*B3 in vitro* at the concentrations used in the assay, for yet undetermined reasons. However, compound **81** exhibited a higher selectivity index than (*S*)-fluoxetine against EV-D68 due to its reduced cytotoxicity. Nevertheless, its inhibitory effect is weaker than that of compounds **16** (dimethylamine moiety, EC_{50} (**16**) = 0.4 μM, SI (**16**) = 110) and **53** (*para*-iodophenoxy moiety, EC_{50} (**53**) = 0.4 μM, SI (**53**) = 58), which have a single modification.

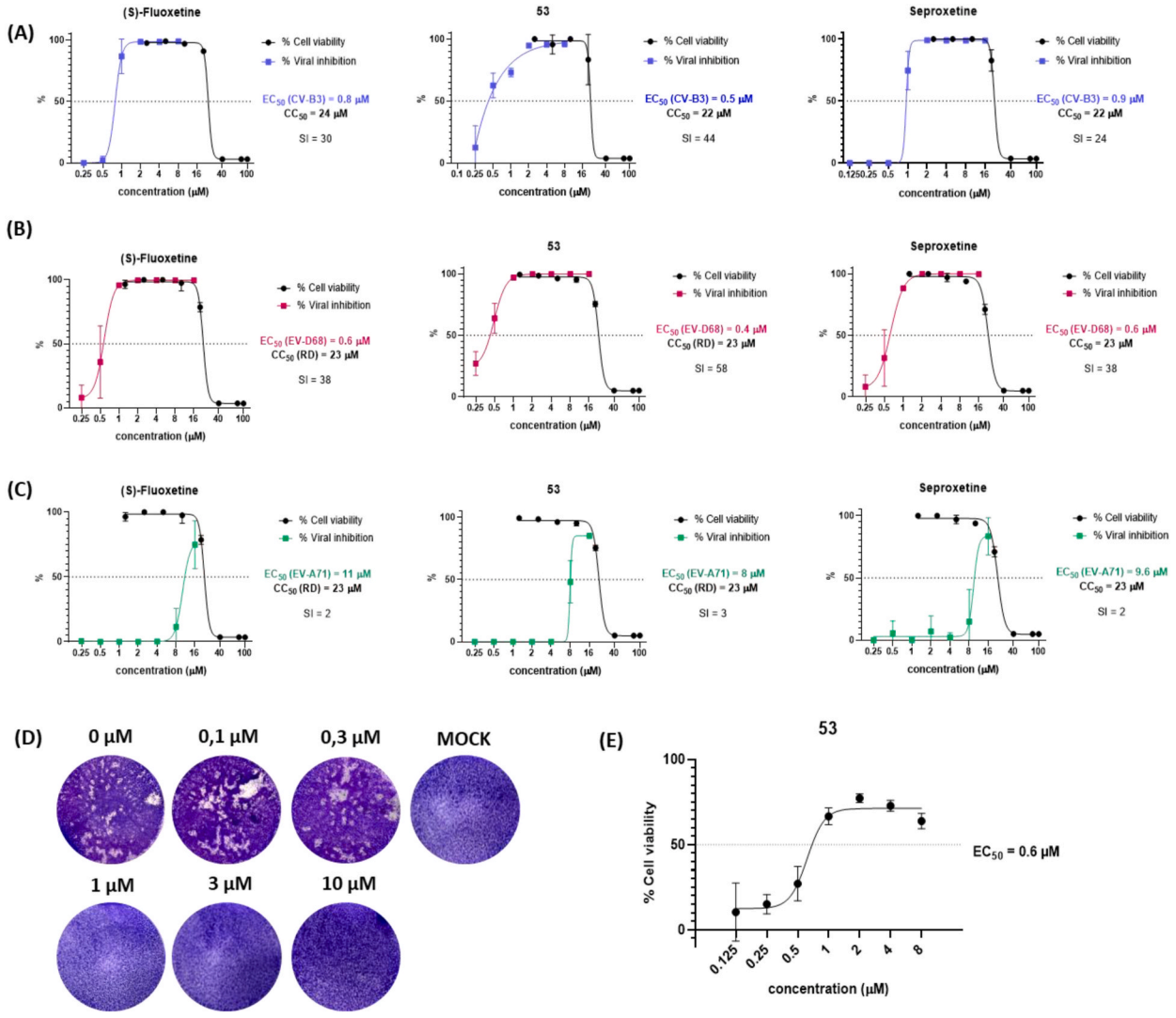

Fig. 3. Antiviral activity of *(S)*-fluoxetine, compound **53** and seproxetine. (**A-C**) Dose-response curves reporting the antiviral activity and cytotoxicity of *(S)*-fluoxetine, compound **53** and seproxetine against CV-B3 in HeLa CCL-2 cells, EV-D68 in RD cells and EV-A71 in RD cells, using virus yield inhibition assay quantified by RT-qPCR. Data presented are from three technical replicates, and error bars represent the mean ± standard deviation. (**D**) Plaque assay images of compound 53 against EV-D68 in RD cells. Images were representatives of two independent replicates. (**E**) Dose-response curve reporting the antiviral activity of compound 53 against EV-D68 in RD cells, using cytopathic effect (CPE) assay.

Table 3
In vitro antiviral activity and cytotoxicity of compounds **16, 18, 22, 31, 53,** seproxetine, (*S*)-fluoxetine, vapendavir and A-967079 against EV-D68 and EV-A71 in RD cells.

Virus/Cell line	EV-D68/RD			EV-A71/RD		
Compounds	EC_{50} (µM) EV-D68	CC_{50} (µM) RD	SI EV-D68	EC_{50} (µM) EV-A71	CC_{50} (µM) RD	SI EV-A71
16	0.4	44	110	–	44	–
18	1.1	41	37	–	41	–
22	0.4	25	63	–	25	–
31	0.5	47	94	–	47	–
53	0.4	23	58	8	23	3
Seproxetine	0.6	23	38	9.6	23	2
(S)-Fluoxetine	0.6	23	38	11	23	2
Vapendavir	ND	>50	ND	1.2	>50	>42
A-967079	0.5	93	186	ND	93	ND

SI: selectivity index (CC_{50}/EC_{50}); (−): no antiviral effect in the tested concentration range; ND: not determined.

Similarly, compounds **82** and **83** are less effective at inhibiting EV-D68 replication than (*S*)-fluoxetine, compounds **18** and **53**, and seproxetine. Compound **84**, however, exhibits comparable potency to (*S*)-fluoxetine and compound **53** in inhibiting EV-D68, but is twice as cytotoxic.

2.5. ADMET prediction for analogue **53** and (S)-fluoxetine

Pharmacokinetics properties of a compound play a crucial role in pharmaceutical toxicology as it deals with the evaluation of the absorption, distribution, metabolism and elimination (ADME) of the molecule in the living organism. Up to day, many statistical methods have been developed that allow the prediction of several ADME-Tox parameters. In this study, we used three online tools, ADMETlab3.0 (https://admetlab3.scbdd.com), Way2Drug (https://way2drug.com/dr/) and FAME3R (https://nerdd.univie.ac.at/fame3r) to evaluate pharmacokinetics parameters and drug-likeness of (*S*)-fluoxetine and compound **53**.

Both compounds present good physicochemical properties with an attractive value of quantitative estimate of drug-likeness (QED) of 0.85 and 0.78 for (*S*)-fluoxetine and analogue **53** respectively, and no

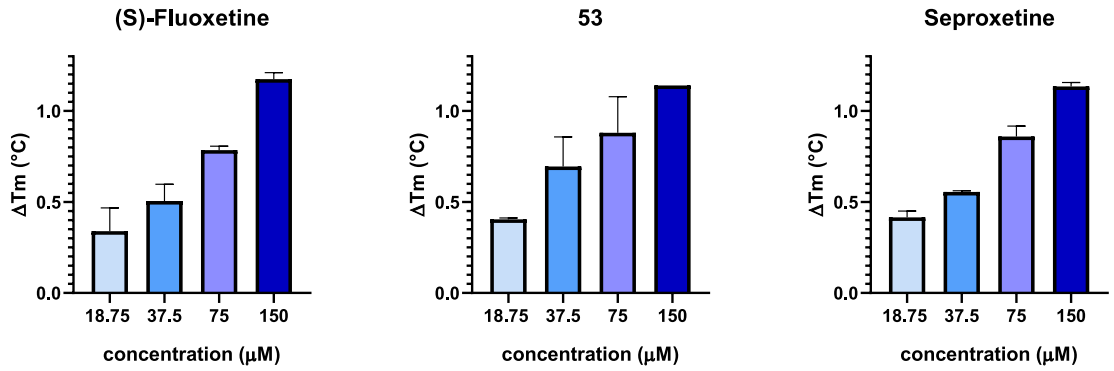

Fig. 4. Compound concentration-dependent increase in the T_m of the CV-B3 Δ36-2C protein with compound **53**, seproxetine and (*S*)-fluoxetine, by thermal shift assay (n = 2 independent replicates).

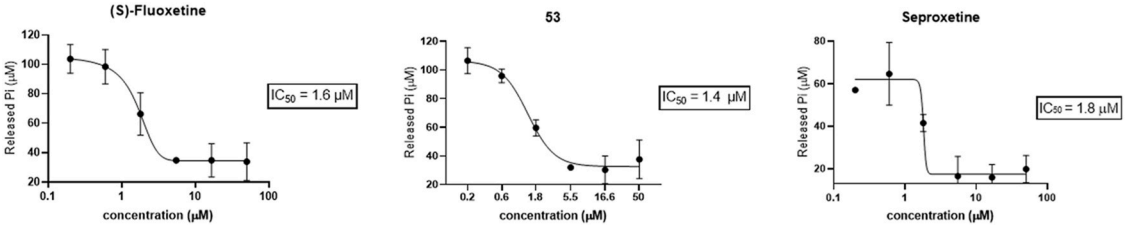

Fig. 5. Biochemical ATPase assays with the CV-B3 hexΔ116-2C protein and compounds **53**, seproxetine and (*S*)-fluoxetine. Data presented are from two technical replicates, and error bars show mean ± standard deviation.

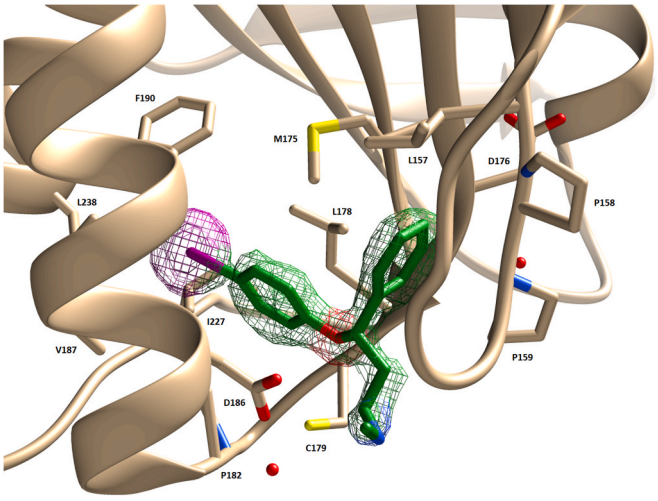

Fig. 6. Crystal structure of 2C CV-B3 protein in complex with compound **53** (PDB ID: 9RQK). 2C protein is displayed in cartoon representation and compound **53** in cylinder representation green carbon atom. Nitrogen, oxygen and iodide are colored in blue, red, and purple, respectively. Small red spheres represent water molecules around the binding sites. Amino acid residues indicated are those establishing van der Waals interactions with compound **53**. The 2Fo-Fc electron density map is shown as a multicolored mesh contoured at 1.6σ around the compound **53**.

violation of the Lipinski's rule of five (Fig. 7A). The human liver microsomal stability is evaluated as stable for both compounds by the ADMETLab3.0 server, which is confirmed by the MetStab tool (https://way2drug.com/metastab/) of the Way2Drug server. On the other hand, the liver microsomal stability of both compounds is evaluated as unstable in mouse or rat species (Fig. 7A and B).

Predictive models of CYP450 bring out a *N*-demethylation of the molecules, as assessed by the tool FAME3R of the OpenRiskNet project (Fig. 7C). Moreover, norfluoxetine is a major metabolite produced by the *N*-demethylation of fluoxetine by CYP2D6 and CYP2C19.

3. Conclusion

To improve the potency of (*S*)-fluoxetine, identified through drug repositioning as an attractive starting point for inhibitory design that binds to an allosteric site on the CV-B3 2C ATPase domain, we employed rational design, X-ray crystallographic structures and computational docking. Our efforts to optimize interactions within the binding pocket enabled us to synthetize novel fluoxetine derivatives that can inhibit CV-B3 and EV-D68 viruses at low to sub-micromolar concentrations. Compounds **16**, **22**, **31** and **81** exhibit slightly higher inhibition effect and selectivity index against EV-D68, while the most potent inhibitor, compound **53**, containing a single modification with an iodide atom, displays higher inhibitory effects and selectivity indexes (CV–B3 EC_{50} = 0.5 μM, SI = 44 and EV-D68 EC_{50} = 0.4 μM, SI = 58) against CV-B3 and EV-D68 than (*S*)-fluoxetine. Furthermore, compound **53** efficiently inhibits CV-B3 ATPase activity (IC_{50} = 1.4 μM) and exhibits a binding mode similar to that of (*S*)-fluoxetine in the expected binding site, validating a suitable allosteric site for the development of new anti-enterovirus agents targeting the 2C protein.

4. Experimental section

4.1. Chemistry

All commercial reagents and solvents were purchased from Sigma Aldrich (Merck), Doug Discovery, Enamine and BLDpharm companies. Furthermore, all dry solvents were obtained via Sigma Aldrich with Sure/Seal™ system and regular solvents were obtained via Sigma Aldrich at technical grade. Analytical thin layer chromatography (TLC) of the reactions was performed on silica gel 60F 254 aluminium plates (Merck) of 0.2 mm thickness with appropriate solvents. The spots were examined with UV light (λ = 254 nm) and Ninhydrin Spray. Preparative flash column chromatographies were performed using silica gel (Merck) G60 230–240 under compressed air or using a Flash Chromatography

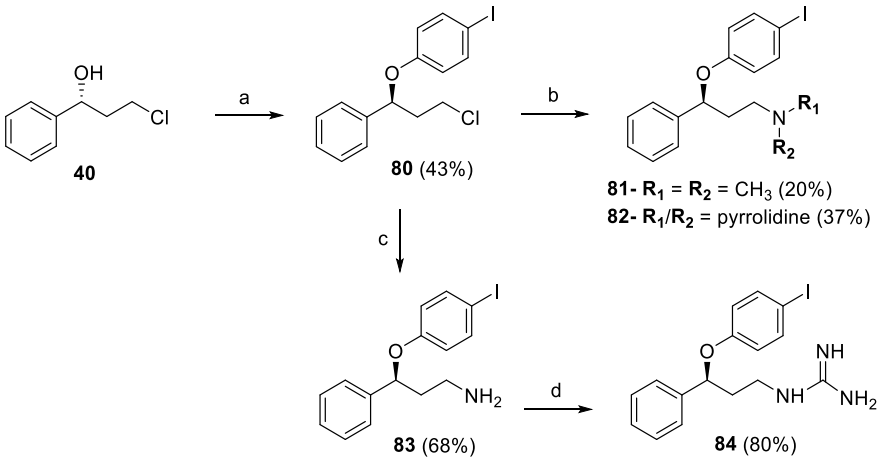

Reagents and conditions: (a) 4-iodophenol, PPh_3, DIAD, dry THF, rt, 16h; (b) NaI, dry THF, 70°C, 16h then amine derivative, rt, 10-20h; (c) potassium phtalimide, dry DMF, 90°C, 4h; then $NH_2NH_2.H_2O$, EtOH, reflux, 3h; (d) 1H-pyrazole-1-carboxamidine hydrochloride, DIEA, dry DMF, rt, 16h.

Scheme 5. Synthesis of analogues **81–84** via a Mitsunobu reaction.

Table 4
In vitro antiviral activity and cytotoxicity of compounds **81–84** against CV-B3 (HeLa CCL-2 cells) and EV-D68 (RD cells).

Virus/Cell line	CVB3/Hela CCL-2			EV-D68/RD		
Compounds	EC_{50} (μM) CV-B3	CC_{50} (μM) HeLa CCL-2	SI CV-B3	EC_{50} (μM) EV-D68	CC_{50} (μM) RD	SI EV-D68
(*S*)-Fluoxetine	0.8	24	30	0.6	23	38
81	–	40	–	0.9	48	53
82	2	14	7	1	24	24
83	1	12	12	1.9	16	8
84	1	17	17	0.5	9	18

SI: selectivity index (CC_{50}/EC_{50}); (−): no antiviral effect in the tested concentration range. To calculate these parameters, a non-linear regression was performed as described in the Methods section, using triplicates for each compound.

Purification System Biotage® Isolera™ One (Interchim puriFlash silica std 20 μm columns). The ^{1}H NMR, ^{19}F NMR and ^{13}C NMR spectra were determined with a BRUKER Avance III nanobay 400 MHz. The chemical shifts are reported in ppm and coupling constants (*J*) are reported in hertz. Reaction monitoring and purity of compounds were recorded by using analytical Thermo Scientific Vanquish® ultra high-performance liquid chromatography (RP-HPLC column Thermo Hypersil Gold® C18 1.9 μm (2.1 × 50 mm); Mobile phase (A: 0.1 % FA H_2O, B: 0.1 % FA MeOH, Time/%B: 0/5, 5/100, 7/100, 7/5, 10/5); Flow rate 0.4 mL/min with DAD at 230 nM. All tested compounds yielded data consistent with a purity of ≥95 %. Low-resolution mass spectra were obtained with a single quadrupole mass spectrometer Thermo Scientific MSQ Plus® or Thermo Scientific ISQ EC® in positive and/or negative electrospray modes. Resolution Mass Spectra (HRMS) were obtained on a SYNAPT G2-S WATERS mass spectrometer. Chiral HPLC analysis for ee determination was performed on an Agilent 1260 Infinity unit (pump G1311B, autosampler G1329B, DAD G1315D) and Agilent OpenLAB Chemstation using method 1: Lux-Amylose-1 column (250 × 4.6, 5 mm), isocratic heptane/isopropanol with 0.1 % diethylamine (95–5) and flow 1 mL/min; method 2: Chiralpak IK column (250 × 4.6, 5 mm), isocratic heptane/isopropanol with 0.1 % diethylamine (90/10) and flow 1 mL/min.

*4.1.1. Synthesis of (S)-3-iodo-1-phenylpropan-1-ol **2***

To a solution of (*S*)-3-Chloro-1-phenyl-1-propanol **1** (2 g, 11.7 mmol, 1 eq) in acetone (100 mL) was added sodium iodide (17.6 mmol, 1.5 eq). The mixture was heated to reflux temperature for 72 h. After the solution was cooled to room temperature, the solvent was evaporated *in vacuo*. The residue was extracted with diethyl ether, the organic layer was washed twice with water, once with brine, dried over Na_2SO_4, and evaporated *in vacuo* to afford a crude residue **2** as pale-beige solid (2.85 g, 93 %) which does not require further purification.

^{1}H RMN (400 MHz, acetone-d6) δ 7.41–7.37 (m, 2H), 7.36–7.31 (m, 2H), 7.27–7.23 (m, 1H), 4.77 (dt, *J* = 7.8, 4.3 Hz, 1H), 4.49 (dd, *J* = 4.3, 0.7 Hz, 1H), 3.38 (dt, *J* = 9.5, 7.7 Hz, 1H), 3.28 (ddd, *J* = 9.6, 7.7, 5.6 Hz, 1H), 2.24–2.11 (m, 2H). ^{13}C RMN (101 MHz, acetone-d6) δ 143.09, 126.30, 125.19, 123.81, 71.13, 41.68, 0.89.

*4.1.2. General procedure for the synthesis of amine derivatives **3–15***

To a solution of (*S*)-3-iodo-1-phenyl-1-propanol **2** (0.76 mmol, 1eq) in dry THF (5 mL) was added the corresponding amine derivative (3.8 mmol, 5 eq). The mixture was stirred under argon atmosphere at room temperature during 3–24h. After completion of the reaction, the solvent was evaporated *in vacuo*. The residue was extracted with dichloromethane, the organic layer was washed twice with water, once with brine, dried over Na_2SO_4, and evaporated *in vacuo*. Crude was purified by column chromatography eluting with dichloromethane-methanol (100–90:10) to give derivatives **3–15**.

*4.1.2.1. (1S)-3-(dimethylamino)-1-phenylpropan-1-ol **3**.* ^{1}H RMN (400 MHz, $CDCl_3$) δ 7.39–7.30 (m, 4H), 7.22–7.17 (tt, *J* = 7.0, 1.6 Hz, 1H), 5.83 (bs, 1H), 4.92 (dd, *J* = 7.7, 4.0 Hz, 1H), 2.70 (ddd, *J* = 12.8, 8.5, 4.8 Hz, 1H), 2.54 (ddd, *J* = 12.6, 5.6, 4.4 Hz, 1H), 2.34 (s, 6H), 1.89–1.82 (m, 2H). LC/MS (ESI): 180.4 $[M+H]^+$; yellow oil. Yield = 36 %.

*4.1.2.2. (1S)-3-(diethylamino)-1-phenylpropan-1-ol **4**.* ^{1}H RMN (400 MHz, $CDCl_3$) δ 7.35–7.24 (m, 4H), 7.22–7.17 (m, 1H), 4.89 (dd, *J* = 7.9, 4.5 Hz, 1H), 3.07–2.81 (m, 6H), 2.01 (m, 2H), 1.23 (t, *J* = 7.3 Hz, 6H). LC/MS (ESI): 208.5 $[M+H]^+$; light yellow oil. Yield = 48 %.

*4.1.2.3. (1S)-1-phenyl-3-(pyrrolidin-1-yl)propan-1-ol **5**.* ^{1}H RMN (400 MHz, $CDCl_3$) δ 7.32–7.24 (m, 4H), 7.20–7.15 (m, 1H), 4.89 (dd, *J* = 8.6, 3.6 Hz, 1H), 3.01–2.92 (m, 1H), 2.91–2.84 (m, 3H), 2.84–2.77 (m, 2H), 2.00–1.90 (m, 2H), 1.89–1.84 (m, 4H). ^{13}C RMN (101 MHz,

(A)

Name	MW	QED	Ro5 violation	calc logD (pH=7.4)	calc logP	Probability HLM instability
(*S*)-fluoxetine	309.13	0.85	0.00	3.28	4.03	0.02
53	367.04	0.78	0.00	3.42	4.19	0.02

(B)

Name\Species	Human	Mouse	Rat
(*S*)-fluoxetine	stable	unstable	unstable
53	stable	unstable	unstable

(C)

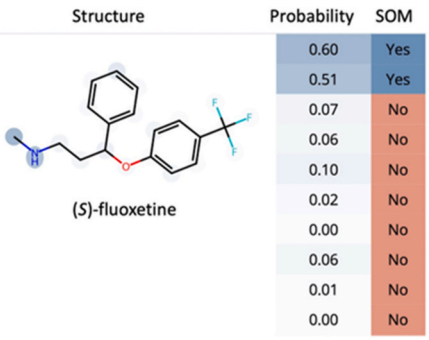

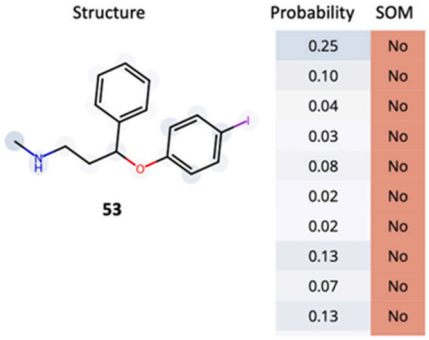

Fig. 7. Prediction of ADME-Tox parameters (**A**) from ADMETLab3.0 server, focused on the molecular weight (MW), the quantitative estimation of drug-likeness (QED), the number of violations of the Lipinski's rule of five, the calculated logD and logP and the predicted probability of the human liver microsomal instability, (**B**) from the MetaStab tool of Way2Drug server, which provides an *in silico* prediction of metabolic stability for three species, human, mouse and rat and (**C**) from FAME3R, a machine learning models for site-of-metabolism (SOM) prediction.

$CDCl_3$) δ 144.62, 128.31, 127.11, 125.58, 74.19, 54.24, 54.02, 35.46, 23.42. LC/MS (ESI): 206.3 $[M+H]^+$; light yellow oil. Yield = 65 %.

4.1.2.4. (1S)-1-phenyl-3-(piperidin-1-yl)propan-1-ol ***6***. ^1H RMN (400 MHz, $CDCl_3$) δ 7.34–7.23 (m, 4H), 7.22–7.16 (m, 1H), 4.90 (dd, *J* = 7.2, 4.9 Hz, 1H), 3.03–2.59 (m, 6H), 2.08–1.94 (m, 2H), 1.90–1.73 (m, 4H), 1.58–1.44 (m, 2H). LC/MS (ESI): 219.9 $[M+H]^+$; light orange oil. Yield = 54 %.

4.1.2.5. (1S)-3-(morpholin-4-yl)-1-phenylpropan-1-ol ***7***. ^1H RMN (400 MHz, $CDCl_3$) δ 7.33–7.25 (m, 4H), 7.22–7.16 (m, 1H), 4.92 (t, *J* = 6.1 Hz, 1H), 3.94–3.78 (m, 4H), 2.98–2.68 (m, 6H), 2.01 (dd, *J* = 12.0, 6.0 Hz, 2H). LC/MS (ESI): 221.2 $[M+H]^+$; light yellow oil. Yield = 59 %.

4.1.2.6. (1S)-3-(4-methylpiperazin-1-yl)-1-phenylpropan-1-ol ***8***. ^1H RMN (400 MHz, $CDCl_3$) δ 7.27 (d, *J* = 4.4 Hz, 4H), 7.21 (dd, *J* = 8.4, 4.3 Hz, 1H), 4.87 (t, *J* = 6.1 Hz, 1H), 3.36–2.81 (m, 10H), 2.63 (s, 3H), 1.95 (bd, *J* = 5.5 Hz, 2H). LC/MS (ESI): 235.3 $[M+H]^+$; light yellow oil. Yield = 60 %.

4.1.2.7. (1S)-3-{[2-(dimethylamino)ethyl](methyl)amino}-1-phenylpropan-1-ol ***9***. ^1H RMN (400 MHz, $CDCl_3$) δ 7.34–7.24 (m, 4H), 7.21–7.16 (m, 1H), 4.88–4.83 (m, 1H), 3.12–3.03 (m, 1H), 2.99–2.81 (m, 5H), 2.68 (s, 6H), 2.42 (s, 3H), 1.95–1.88 (m, 2H). LC/MS (ESI): 237.4 $[M+H]^+$; light yellow oil. Yield = 47 %.

4.1.2.8. (1S)-3-(imidazole-1-yl)-1-phenylpropan-1-ol ***10***. ^1H RMN (400 MHz, $CDCl_3$) δ 7.88 (bs, 1H), 7.35–7.28 (m, 4H), 7.28–7.23 (m, 1H), 7.03 (bs, 1H), 6.97 (t, *J* = 1.2 Hz, 1H), 4.54 (dd, *J* = 9.1, 4.1 Hz, 1H), 4.28 (ddd, *J* = 14.1, 8.6, 6.7 Hz, 1H), 4.08 (ddd, *J* = 13.9, 6.9, 4.9 Hz, 1H), 2.2–2.04 (m, 2H). ^{13}C NMR (101 MHz, $CDCl_3$) δ 144.04, 137.17, 128.61, 127.75, 127.43, 125.71, 119.23, 70.15, 44.23, 39.77. LC/MS (ESI): 203.4 $[M+H]^+$; colorless oil. Yield = 83 %.

4.1.2.9. (1S)-3-(benzylamino)-1-phenylpropan-1-ol ***11***. ^1H RMN (400 MHz, $CDCl_3$) δ 7.41–7.31 (m, 8H), 7.32–7.24 (m, 2H), 4.99 (dd, *J* = 8.5, 2.6 Hz, 1H), 3.88 (d, J = 13.1, Hz, 1H), 3.83 (d, J = 13.1, Hz, 1H), 3.07–2.99 (m, 1H), 2.98–2.89 (m, 1H), 2.01–1.93 (m, 1H), 1.89–1.78 (m, 1H). ^{13}C RMN (101 MHz, $CDCl_3$) δ 144.91, 138.86, 128.61, 128.38, 128.24, 127.42, 126.96, 125.59, 75.53, 53.75, 47.72, 37.20. LC/MS (ESI): 242.17 $[M+H]^+$; yellow oil. Yield = 68 %.

4.1.2.10. (1S)-1-phenyl-3-((pyridin-2-ylmethyl)amino)propan-1-ol ***12***. ^1H NMR (400 MHz, $CDCl_3$) δ 8.48 (ddd, *J* = 4.8, 1.5, 0.8 Hz, 1H), 7.60 (td, *J* = 7.7, 1.8 Hz, 1H), 7.31–7.20 (m, 5H), 7.18–7.12 (m, 2H), 4.93 (dd, *J* = 8.5, 3.3 Hz, 1H), 3.98 (bs, 2H), 3.06–2.89 (m, 2H), 2.04–1.95 (m, 1H), 1.95–1.83 (m, 1H). ^{13}C RMN (101 MHz, $CDCl_3$) δ 155.58, 149.42, 144.30, 137.01, 128.31, 127.17, 125.63, 122.93, 122.87, 74.14, 53.43, 47.16, 36.28. LC/MS (ESI): 243.13 $[M+H]^+$; yellow oil. Yield = 73 %.

4.1.2.11. (1S)-1-phenyl-3-(4-phenylpiperazin-1-yl)propan-1-ol ***13***. ^1H RMN (400 MHz, $CDCl_3$) δ 7.34–7.25 (m, 4H), 7.23–7.15 (m, 3H), 6.86 (d, *J* = 8.4 Hz, 2H), 6.81 (t, *J* = 7.3 Hz, 1H), 4.86–4.92 (m, 1H), 3.20 (t, *J* = 4.9 Hz, 4H), 2.81–2.69 (m, 3H), 2.67–2.56 (m, 3H), 1.90–1.82 (m, 2H). ^{13}C RMN (101 MHz, $CDCl_3$) δ 151.00, 144.70, 129.20, 128.29, 127.04, 125.55, 120.15, 116.34, 75.28, 57.01, 53.22, 49.16, 33.67. LC/MS (ESI): 297.25 $[M+H]^+$; light yellow solid. Yield = 85 %.

4.1.2.12. (1S)-3-(4-benzylpiperidin-1-yl)-1-phenylpropan-1-ol ***14***. ^1H RMN (400 MHz, $CDCl_3$) δ 7.32–7.26 (m, 3H), 7.24–7.08 (m, 5H), 7.06 (d, *J* = 7.2 Hz, 2H), 4.86 (dd, *J* = 7.2, 4.2 Hz, 1H), 3.09 (d, *J* = 11.1 Hz, 1H), 3.02 (d, *J* = 11.0 Hz, 1H), 2.68–2.59 (m, 1H), 2.58–2.50 (m, 1H), 2.47 (d, *J* = 7.0 Hz, 2H), 2.02 (t, *J* = 11.5 Hz, 1H), 1.89–1.76 (m, 3H), 1.68–1.58 (m, 2H), 1.57–1.44 (m, 1H), 1.43–1.29 (m, 2H). ^{13}C RMN (101 MHz, $CDCl_3$) δ 144.89, 140.33, 129.10, 128.28, 128.24, 126.94, 125.97, 125.56, 74.84, 56.90, 54.56, 53.09, 42.90, 37.64, 33.70, 31.88, 31.58. LC/MS (ESI): 310.23 $[M+H]^+$; light orange oil. Yield = 90 %.

4.1.2.13. (1S)-3-(4-benzylpiperazin-1-yl)-1-phenylpropan-1-ol ***15***. ^1H RMN (400 MHz, $CDCl_3$) δ = 7.31–7.26 (m, 3H), 7.25. – 7.21 (m, 5H), 7.20–7.13 (m, 2H), 4.85 (dd, J = 6.8 and 4.6 Hz, 1H), 3.44 (s, 2H), 2.66–2.31 (m, 10H), 1.82–1.72 (m, 2H). ^{13}C RMN (101 MHz, $CDCl_3$) δ = 144.94, 137.95, 129.22, 128.29, 128.23, 127.16, 126.92, 125.55, 75.51, 62.95, 56.98, 53.04, 45.69, 33.64. LC/MS (ESI): 311.29 $[M+H]^+$; light

orange oil. Yield = 27 %.

*4.1.3. General procedure for synthesis of benzotrifluoride derivatives **16–28, 31–32** and trifluoromethylpyridine derivative **62** via a SNAr reaction*

A mixture of NaH (3 eq) and the corresponding amine derivative (1eq, **3–15**, **29–30** and **61**) in dry DMF (~5 mL) was stirred under argon at 60 °C for 1h. Then, 1-chloro-4-(trifluoromethyl)benzene (1.2 eq, for **16–28** and **31–32**) or 2-chloro-5-(trifluoromethyl)pyridine (1.2 eq, for **62**) was added and the mixture was heated to 100 °C for 2–5h. After being cooled at room temperature, the reaction mixture was diluted in DCM and the organic layers was washed three times with water, once with brine, dried over Na_2SO_4, and evaporated *in vacuo*. Crude was purified by column chromatography eluting with dichloromethane-methanol (100–95:5) to give derivatives **16–17**, **19–26**, **31–32** and **62** or AcOEt/Cyclohexane (20/80 to 80/20) to give derivatives **18** and **27–28**.

*4.1.3.1. Dimethyl[(3S)-3-phenyl-3-[4-(trifluoromethyl)phenoxy]propyl] amine **16**.* ^{1}H RMN (400 MHz, $CDCl_3$) δ 7.42 (d, J = 8.5 Hz, 2H), 7.36–7.32 (m, 4H), 7.29–7.25 (m, 1H), 6.90 (d, J = 8.5 Hz, 2H), 5.31 (dd, J = 8.2, 4.8 Hz, 1H), 2.65–2.50 (m, 2H), 2.36 (s, 6H), 2.31–2.18 (m, 1H), 2.13–2.04 (m, 1H). ^{13}C RMN (101 MHz, $CDCl_3$) δ 160.06, 139.81, 129.00, 128.27, 126.85 (q, $^3J_{CF}$ = 3.7 Hz), 125.76, 124.29 (q, $^1J_{CF}$ = 271.2 Hz), 123.20 (q, $^2J_{CF}$ = 32.7 Hz), 115.76, 77.75, 55.28, 44.20, 34.77. ^{19}F RMN (376 MHz, $CDCl_3$) δ −61.73. LC/MS (ESI): 324.2 $[M+H]^+$; HRMS (TOF, ESI+) cald for C18H20F3NO [M+H]+ 324.157, found 324.157; Chiral analytical analysis, method 1: RT, 4.02 min, 93 % ee; Light yellow oil. Yield = 17 %.

*4.1.3.2. Diethyl[(3S)-3-phenyl-3-[4-(trifluoromethyl)phenoxy]propyl] amine **17**.* ^{1}H RMN (400 MHz, $CDCl_3$) δ 7.38 (d, J = 8.6 Hz, 2H), 7.32–7.27 (m, 4H), 7.27–7.22 (m, 1H), 6.83 (d, J = 8.5 Hz, 2H), 5.41 (dd, J = 8.4, 3.9 Hz, 1H), 3.25–3.00 (m, 6H), 2.53–2.42 (m, 1H), 2.42–2.30 (m, 1H), 1.34 (t, J = 7.3 Hz, 3H), 1.31 (t, J = 7.3 Hz, 3H). ^{13}C RMN (101 MHz, $CDCl_3$) δ 160.35, 140.49, 128.87, 128.03, 126.76 (q, $^3J_{CF}$ = 3.7 Hz), 125.80, 124.35 (q, $^1J_{CF}$ = 271.1 Hz), 122.94 (q, $^2J_{CF}$ = 32.7 Hz), 115.73, 78.17, 48.52, 46.93, 34.96, 10.65. ^{19}F RMN (376 MHz, $CDCl_3$) δ −61.68. LC/MS (ESI): 352.2 $[M+H]^+$; HRMS (TOF, ESI+) cald for C20H24F3NO $[M+H]^+$ 352.187, found 352.1883; colorless oil. Yield = 34 %.

*4.1.3.3. 1-[(3S)-3-phenyl-3-[4-(trifluoromethyl)phenoxy]propyl]pyrrolidine **18**.* ^{1}H RMN (400 MHz, $CDCl_3$) δ 7.36 (d, J = 8.6 Hz, 2H), 7.29–7.24 (m, 4H), 7.24–7.20 (m, 1H), 6.83 (d, J = 8.6 Hz, 2H), 5.27 (dd, J = 8.1, 4.7 Hz, 1H), 2.78–2.62 (m, 6H), 2.31–2.20 (m, 1H), 2.19–2.09 (m, 1H), 1.8–1.78 (m, 4H). ^{13}C RMN (101 MHz, $CDCl_3$) δ 160.37, 140.43, 128.86, 128.02, 126.79 (q, $^3J_{CF}$ = 3.6 Hz), 125.82, 124.35 (q, $^1J_{CF}$ = 271.1 Hz), 122.92 (q, $^2J_{CF}$ = 32.7 Hz), 115.77, 78.28, 54.12, 52.44, 36.86, 23.49. ^{19}F RMN (376 MHz, $CDCl_3$) δ −61.70. LC/MS (ESI): 349.2 $[M+H]^+$; HRMS (TOF, ESI+) cald for C20H22F3NO $[M+H]^+$ 350.1726, found 350.1726; light orange oil. Yield = 75 %.

*4.1.3.4. 1-[(3S)-3-phenyl-3-[4-(trifluoromethyl)phenoxy]propyl]piperidine **19**.* ^{1}H RMN (400 MHz, $CDCl_3$) δ 7.36 (d, J = 8.6 Hz, 2H), 7.29–7.25 (m, 4H), 7.22–7.21 (m, 1H), 6.83 (d, J = 8.5 Hz, 2H), 5.29 (dd, J = 7.9, 4.8 Hz, 1H), 2.78–2.54 (m, 6H), 2.38–2.18 (m, 2H), 1.84–1.69 (m, 4H), 1.53–1.41 (m, 2H). ^{13}C RMN (101 MHz, $CDCl_3$) δ 160.22, 140.05, 128.90, 128.14, 126.82 (q, $^3J_{CF}$ = 3.7 Hz), 125.79, 124.31 (q, $^1J_{CF}$ = 271.1 Hz), 123.08 (q, $^2J_{CF}$ = 32.4 Hz), 115.74, 78.26, 54.85, 54.10, 34.28, 24.27, 23.28. ^{19}F RMN (376 MHz, $CDCl_3$) δ −61.70. LC/MS (ESI): 364.2 $[M+H]^+$; HRMS (TOF, ESI+) cald for C21H24F3NO $[M+H]^+$ 364.188, found 364.1883 orange oil. Yield = 13 %.

*4.1.3.5. 4-[(3S)-3-phenyl-3-[4-(trifluoromethyl)phenoxy]propyl]morpholine **20**.* ^{1}H RMN (400 MHz, $CDCl_3$) 7.36 (d, J = 8.6 Hz, 2H), 7.27 (bd, J = 4.4 Hz, 2H), 7.23–7.20 (m, 1H), 6.83 (d, J = 8.5 Hz, 1H), 5.25 (dd, J = 8.0, 4.9 Hz, 1H), 3.83–3.63 (m, 4H), 2.70–2.37 (m, 6H), 2.29–2.16 (m, 1H), 2.12–2.01 (m, 1H). ^{13}C RMN (101 MHz, $CDCl_3$) δ 160.24, 140.24, 128.93, 128.17, 126.83 (q, $^3J_{CF}$ = 3.7 Hz), 125.79, 124.31 (q, $^1J_{CF}$ = 271.3 Hz), 123.10 (q, $^2J_{CF}$ = 32.5 Hz), 115.74, 78.10, 65.73, 54.90, 53.16, 34.36. ^{19}F RMN (376 MHz, $CDCl_3$) δ −61.61. LC/MS (ESI): 366.2 $[M+H]^+$; HRMS (TOF, ESI+) cald for $C_{20}H_{22}F_3NO_2$ $[M+H]^+$ 366.167, found 366.1675; light yellow oil. Yield = 39 %.

*4.1.3.6. 1-Methyl-4-[(3S)-3-phenyl-3-[4-(trifluoromethyl)phenoxy]propyl]piperazine **21**.* ^{1}H RMN (400 MHz, $CDCl_3$) 7.36 (d, J = 8.6 Hz, 2H), 7.29–7.24 (m, 4H), 7.23–7.20 (m, 1H), 6.82 (d, J = 8.6 Hz, 2H), 5.20 (dd, J = 8.1, 4.9 Hz, 1H), 2.74–2.53 (m, 8H), 2.52 (t, J = 7.2 Hz, 2H), 2.39 (s, 3H), 2.21–2.09 (m, 1H), 2.03–1.92 (m, 1H). ^{13}C RMN (101 MHz, $CDCl_3$) δ 160.50, 140.70, 128.84, 127.99, 126.77 (q, $^3J_{CF}$ = 3.7 Hz), 125.81, 124.35 (q, $^1J_{CF}$ = 271.2 Hz), 122.89 (q, $^2J_{CF}$ = 32.7 Hz), 115.74, 78.41, 54.37, 54.06, 51.75, 45.04, 35.63. ^{19}F RMN (376 MHz, $CDCl_3$) δ −61.72. LC/MS (ESI): 379.1 $[M+H]^+$; HRMS (TOF, ESI+) cald for C21H25F3N2O $[M+H]^+$ 379.199, found/; colorless oil. Yield = 17 %.

*4.1.3.7. [2-(dimethylamino)ethyl](methyl)[(3S)-3-phenyl-3-[4-(trifluoromethyl)phenoxy]propyl]amine **22**.* ^{1}H RMN (400 MHz, $CDCl_3$) 7.35 (d, J = 8.6 Hz, 2H), 7.32–7.23 (m, 4H), 7.23–7.17 (m, 1H), 6.84 (d, J = 8.6 Hz, 2H), 5.27 (dd, J = 8.6, 4.4 Hz, 1H), 2.63–2.35 (m, 6H), 2.23 (s, 6H), 2.22 (s, 3H), 2.15–2.04 (m, 1H), 1.99–1.90 (m, 1H). ^{13}C RMN (101 MHz, $CDCl_3$) δ 159.62, 140.05, 127.76, 126.81, 125.73 (q, $^3J_{CF}$ = 3.7 Hz), 124.82, 123.35 (q, $^1J_{CF}$ = 271.0 Hz), 121.73 (q, $^2J_{CF}$ = 32.7 Hz), 114.74, 77.11, 55.67, 53.96, 52.94, 44.08, 41.20, 35.24. ^{19}F RMN (376 MHz, $CDCl_3$) δ −61.60. LC/MS (ESI): 381.2 $[M+H]^+$; HRMS (TOF, ESI+) cald for C21H27F3N2O $[M+H]^+$ 381.215, found 381.2148; colorless oil. Yield = 26 %.

*4.1.3.8. 1-[(3S)-3-phenyl-3-[4-(trifluoromethyl)phenoxy]propyl]imidazole **23**.* ^{1}H RMN (400 MHz, $CDCl_3$) 8.21 (bs, 1H), 7.36 (d, J = 8.6 Hz, 2H), 7.30–7.18 (m, 6H), 6.99 (m, 1H), 6.79 (d, J = 8.6 Hz, 2H), 5.07 (dd, J = 9.0, 3.7 Hz, 1H), 4.37–4.18 (m, 2H), 2.49–2.38 (m, 1H), 2.31 (m, 1H). ^{13}C RMN (101 MHz, $CDCl_3$) δ 158.70, 138.47, 138.37, 128.08, 127.80, 127.40, 125.93 (q, $^3J_{CF}$ = 3.7 Hz), 125.40, 124.62, 123.19 (q, $^1J_{CF}$ = 271.1 Hz), 122.39 (q, $^2J_{CF}$ = 32.7 Hz), 114.66, 75.77, 43.59, 38.63. ^{19}F RMN (376 MHz, $CDCl_3$) δ −61.72. LC/MS (ESI): 347.0 $[M+H]^+$; HRMS (TOF, ESI+) cald for C19H17F3N2O $[M+H]^+$ 347.1366, found 347.1366; colorless oil. Yield = 43 %.

*4.1.3.9. Benzyl[(3S)-3-phenyl-3-[4-(trifluoromethyl)phenoxy]propyl] amine **24**.* ^{1}H RMN (400 MHz, $CDCl_3$) δ 7.35 (d, J = 8.6 Hz, 2H), 7.26–7.20 (m, 7H), 7.20–7.13 (m, 3H), 6.81 (d, J = 8.6 Hz, 2H), 5.27 (dd, J = 8.2, 4.8 Hz, 1H), 3.71 (s, 2H), 2.80–2.60 (m, 2H), 2.26–2.07 (m, 1H), 2.05–1.96 (m, 1H). ^{13}C RMN (101 MHz, $CDCl_3$) δ 160.56, 140.99, 139.70, 128.78, 128.46, 128.23, 127.84, 127.13, 126.75 (q, $^3J_{CF}$ = 3.7 Hz), 125.81, 124.40 (q, $^1J_{CF}$ = 271.0 Hz), 122.79 (q, $^2J_{CF}$ = 32.6 Hz), 115.78, 78.57, 53.81, 45.35 38.68. ^{19}F RMN (376 MHz, $CDCl_3$) δ −61.55. LC/MS (ESI): 386.13 $[M+H]^+$; HRMS (TOF, ESI+) cald for C23H22F3NO $[M+H]^+$ 386.172, found 386.1726; light brown oil. Yield = 27 %.

*4.1.3.10. [(3S)-3-phenyl-3-[4-(trifluoromethyl)phenoxy]propyl](pyridine-2-ylmethyl)amine **25**.* ^{1}H RMN (400 MHz, $CDCl_3$) δ 8.40 (dd, J = 4.8, 0.6 Hz, 1H), 7.54 (td, J = 7.7, 1.7 Hz, 1H), 7.36 (d, J = 8.7 Hz, 2H), 7.25 (t, J = 4.4 Hz, 4H), 7.22–7.17 (m, 2H), 7.10 (dd, J = 7.4, 5.0 Hz, 1H), 6.83 (d, J = 8.7 Hz, 2H), 5.32 (dd, J = 8.3, 4.5 Hz, 1H), 3.92 (s, 2H), 2.91–2.79 (m, 2H), 2.31–2.18 (m,1H), 2.15–2.03 (m,1H). ^{13}C RMN (101 MHz, $CDCl_3$) 160.36, 157.67, 149.29, 140.60, 136.71, 128.83, 127.94, 126.75 (q, $^3J_{CF}$ = 3.7 Hz), 125.79, 125.61 (q,

$^{1}J_{CF}$ = 271.1 Hz), 123.09 (q, $^{2}J_{CF}$ = 32.6 Hz), 122.43, 122.40, 115.82, 78.60, 54.34, 45.70, 38.15. ^{19}F RMN (376 MHz, $CDCl_3$) δ −61.69. LC/MS (ESI): 387.10 $[M+H]^+$; HRMS (TOF, ESI+) cald for C22H21F3N2O $[M+H]^+$ 387.167, found 387.1679; light yellow oil. Yield = 13 %.

4.1.3.11. 1-Phenyl-4-[(3S)-phenyl-3-[4-(trifluoromethyl)phenoxy]propyl] piperazine ***26***. ^{1}H RMN (400 MHz, $CDCl_3$) δ 7.36 (d, *J* = 8.7 Hz, 2H), 7.29–7.27 (m, 4H), 7.23–7.17 (m, 3H), 6.86 (d, *J* = 7.8 Hz, 2H), 6.84 (d, *J* = 8.4 Hz, 2H), 6.80 (t, 7.3 Hz, 1H), 5.26 (dd, *J* = 7.8, 5.0 Hz, 1H), 3.26–3.06 (m, 4H), 2.75–2.46 (m, 6H), 2.40–2.26 (m, 1H), 2.15–1.99 (m, 1H). ^{13}C RMN (101 MHz, $CDCl_3$) δ 160.52, 151.15, 140.70, 129.17, 128.84, 127.99, 126.79 (q, $^{3}J_{CF}$ = 3.7 Hz), 125.87, 125.71 (q, $^{1}J_{CF}$ = 271.1 Hz), 122.90 (q, $^{2}J_{CF}$ = 32.6 Hz), 116.22, 115.77, 78.48, 54.47, 53.12, 48.87, 35.56. ^{19}F RMN (376 MHz, $CDCl_3$) δ −61.59. LC/MS (ESI): 441.17 $[M+H]^+$; HRMS (TOF, ESI+) cald for C26H27F3N2O $[M+H]_+$ 441.215, found 441.2148; light yellow oil. Yield = 20 %.

4.1.3.12. 4-Benzyl-1-[(3S)-phenyl-3-[4-(trifluoromethyl)phenoxy]propyl] piperidine ***27***. ^{1}H RMN (400 MHz, $CDCl_3$) δ 7.35 (d, *J* = 8.6 Hz, 2H), 7.27–7.24 (m, 4H), 7.23–7.19 (m, 3H), 7.16–7.13 (m, 1H), 7.04 (d, *J* = 8.3 Hz, 2H), 6.79 (d, *J* = 8.6 Hz, 2H), 5.34 (dd, *J* = 8.6, 3.8 Hz, 1H), 3.52–3.42 (m, 2H), 3.13–2.96 (m, 2H), 2.61–2.39 (m, 6H), 2.10–1.95 (m, 2H), 1.73 (bd, *J* = 14.8 Hz, 2H), 1.69–1.61 (m, 1H). ^{13}C RMN (101 MHz, $CDCl_3$) δ 159.65, 139.05, 138.86, 129.12, 129.00, 128.55, 128.53, 126.94 (q, $^{3}J_{CF}$ = 3.6 Hz), 126.45, 125.71 (q, $^{1}J_{CF}$ = 271.1 Hz), 125.67, 123.51 (q, $^{2}J_{CF}$ = 32.9 Hz), 115.68, 77.60, 77.23, 54.63, 54.13, 53.43, 52.81, 41.93, 36.65, 32.58. ^{19}F RMN (376 MHz, $CDCl_3$) δ −61.71. LC/MS (ESI): 454.18 $[M+H]^+$; HRMS (TOF, ESI+) cald for C28H30F3NO $[M+H]^+$ 454.235, found 454.2352; light brown oil. Yield = 18 %.

4.1.3.13. 1-Benzyl-4-[(3S)-phenyl-3-[4-(trifluoromethyl)phenoxy]propyl] piperazine ***28***. ^{1}H RMN (400 MHz, $CDCl_3$) δ 7.35 (d, *J* = 8.7 Hz, 2H), 7.27–7.20 (m, 8H), 7.21–7.16 (m, 2H), 6.85–6.80 (d, *J* = 8.7 Hz, 2H), 5.20 (dd, *J* = 8.0, 5.0 Hz, 1H), 3.45 (s, 2H), 2.58–2.31 (m, 10H), 2.15 (td, *J* = 14.6, 7.6 Hz, 1H), 2.01–1.89 (m, 1H). ^{13}C RMN (101 MHz, $CDCl_3$) δ 160.61, 140.91, 137.77, 129.28, 128.77, 128.28, 127.89, 127.20, 126.74 (q, $^{3}J_{CF}$ = 3.5 Hz), 125.87, 125.73 (q, $^{1}J_{CF}$ = 271.1 Hz), 122.95 (q, $^{2}J_{CF}$ = 32.7 Hz), 115.78, 78.64, 62.93, 54.42, 53.06, 52.79, 35.73. ^{19}F RMN (376 MHz, $CDCl_3$) δ −61.59. LC/MS (ESI): 455.18 $[M+H]^+$; HRMS (TOF, ESI+) cald for C27H29F3N2O $[M+H]^+$ 455.230, found 455.2305; light brown oil. Yield = 35 %.

4.1.3.14. Methyl[(3S)-3-(thiophen-2-yl)-3-[4-(trifluoromethyl)phenoxy] propyl]amine ***31***. ^{1}H RMN (400 MHz, MeOD) δ 7.41 (d, *J* = 8.7 Hz, 2H), 7.25 (dd, *J* = 5.1, 1.1 Hz, 1H), 7.04 (bd, *J* = 3.5 Hz, 1H), 6.99 (d, *J* = 8.6 Hz, 2H), 6.87 (dd, *J* = 5.1, 3.5 Hz, 1H), 5.68 (dd, *J* = 7.6, 5.5 Hz, 1H), 2.78–2.62 (m, 2H), 2.34 (s, 3H), 2.30–2.19 (m, 1H), 2.15–2.03 (m, 1H). ^{13}C RMN (101 MHz, MeOD) δ 160.32, 143.68, 126.34 (q, $^{3}J_{CF}$ = 3.7 Hz), 126.27, 124.47 (q, $^{1}J_{CF}$ = 270.3 Hz), 125.47, 125.12, 122.88 (q, $^{2}J_{CF}$ = 32.5 Hz), 116.01, 74.33, 47.10, 37.32, 34.27. ^{19}F RMN (376 MHz, MeOD) δ −63.15. LC/MS (ESI): 316.1 $[M+H]^+$; HRMS (TOF, ESI+) cald for C15H16F3NOS $[M+H]^+$ 316.097, found 316.0977; light yellow oil. Yield = 23 %.

4.1.3.15. Dimethyl[(3S)-3-(thiophen-2-yl)-3-[4-(trifluoromethyl)phenoxy]propyl]amine ***32***. ^{1}H RMN (400 MHz, $CDCl_3$) δ 7.40 (d, *J* = 8.5 Hz, 2H), 7.17 (dd, *J* = 5.0, 1.1 Hz, 1H), 6.97 (dd, *J* = 3.5, 0.5 Hz, 1H), 6.93 (d, *J* = 8.5 Hz, 2H), 6.88 (dd, *J* = 5.0, 3.5 Hz, 1H), 5.58 (dd, *J* = 7.5, 5.6 Hz, 1H), 2.55–2.40 (m, 2H), 2.34–2.21 (m, 1H), 2.27 (s, 6H), 2.16–2.04 (m, 1H). ^{13}C RMN (101 MHz, $CDCl_3$) δ 160.17, 143.72, 126.84 (q, $^{3}J_{CF}$ = 3.7 Hz), 126.78, 125.33, 125.30, 124.32 (q, $^{1}J_{CF}$ = 271.4 Hz), 123.39 (q, $^{2}J_{CF}$ = 32.6 Hz), 115.99, 74.38, 55.24, 44.90, 35.86. ^{19}F RMN (376 MHz, $CDCl_3$) δ −61.62. LC/MS (ESI): 330.2 $[M+H]^+$; HRMS (TOF, ESI+) cald for C16H18F3NOS $[M+H]^+$ 330.1135, found 330.1134; colorless oil. Yield = 71 %.

4.1.3.16. Methyl[(3S)-3-phenyl-3-{[5-(trifluoromethyl)pyridine-2-yl] oxy}propyl]amine ***62***. ^{1}H RMN (400 MHz, $CDCl_3$) δ 8.36 (dd, *J* = 1.3, 0.8 Hz, 1H), 7.64 (dd, *J* = 9.1, 2.4 Hz, 1H), 7.38–7.30 (m, 4H), 7.27–7.22 (m, 1H), 6.56 (d, *J* = 9.1 Hz, 1H), 5.41 (bs, 1H), 4.53 (dd, *J* = 10.5, 2.8 Hz, 1H), 4.37 (ddd, *J* = 15.0, 11.2, 4.3 Hz, 1H), 3.34 (ddd, *J* = 14.6, 5.3, 3.4 Hz, 1H), 3.06 (s, 3H), 2.14–1.99 (m, 1H), 1.92–1.78 (m, 1H). ^{13}C RMN (101 MHz, $CDCl_3$) δ 160.28, 145.42 (q, $^{3}J_{CF}$ = 4.3 Hz), 144.10, 134.82 (q, $^{3}J_{CF}$ = 3.0 Hz), 128.32, 127.14, 125.62, 124.62 (q, $^{1}J_{CF}$ = 270.1 Hz), 114.46 (q, $^{2}J_{CF}$ = 33.2 Hz), 105.11, 69.76, 46.78, 37.69, 36.14. ^{19}F RMN (376 MHz, $CDCl_3$) δ −59.03. LC/MS (ESI): 311.26 $[M+H]^+$; HRMS (TOF, ESI+) cald for C16H17F3N2O $[M+H]^+$ 311.1365, found 311.1366; colorless oil. Yield = 27 %.

4.1.4. Synthesis of tert-butyl N-[(3R)-3-hydroxy-3-phenylpropyl]-N-methylcarbamate ***34***

To a stirred solution of (*R*)-3-(methylamino)-1-phenylpropan-1-ol **33** (1.9 g, 11.51 mmol, 1 eq) in dry DCM (50 mL) was added di-*tert*-butyl dicarbonate (Boc2O, 2.76g, 1.1 eq) at 4 °C. The reaction mixture was stirred at room temperature for 48h, then washed twice with saturated NH_4Cl, once with brine, dried over Na_2SO_4, and evaporated *in vacuo* to afford a crude residue **34** as pale-yellow oil (3.02 g, 98 %) which does not require further purification.

^{1}H RMN (400 MHz, $CDCl_3$) δ 7.31–7.23 (m, 4H), 7.20–7.15 (m, 1H), 4.53 (dd, *J* = 9.9, 3.4 Hz, 1H), 3.77–3.62 (m, 1H), 3.10 (bs, 1H), 3.00 (ddd, *J* = 14.4, 6.1, 4.0 Hz, 1H), 2.79 (s, 3H), 1.92–1.81 (m, 1H), 1.71 (m, 1H), 1.39 (s, 9H). ^{13}C RMN (101 MHz, $CDCl_3$) δ 156.77, 144.18, 128.39, 127.25, 125.66, 80.07, 70.49, 45.35, 37.26, 34.30, 28.42. LC/MS (ESI): 266.1 $[M+H]^+$; light yellow oil. Yield = 98 %.

4.1.5. General procedure for synthesis of derivatives ***35–39*** *via a Mitsunobu reaction followed by an acidic hydrolysis*

To a stirred solution of triphenylphosphine (1.5 eq, 0.85 mmol) in dry THF (2 mL), cooled at 4 °C, was slowly added diisopropyl azodicarboxylate (DIAD, 1.5 eq, 0.85 mmol). After 20 min, the corresponding phenol (1 eq, 0.57 mmol) in dry THF (1 mL) was added and the reaction mixture was stirred 1h at 4 °C. Then, a solution of tert-butyl[(3R)-3-hydroxy-3-phenylpropyl]methylcarbamate **34** (1 eq, 0.57 mmol) in dry THF (0.5 mL) was added 4 °C. The reaction mixture was stirred at room temperature for 4–18h before removing the solvent *in vacuo*. The residue was diluted in DCM, washed twice with water, once with brine, dried over Na_2SO_4, and the solvent was evaporated *in vacuo*. The crude residue was purified by flash column chromatography eluting with DCM/cyclohexane (50:50 to 80:20 or 70:30 to 100:0).

The obtained residue was then solubilized in DCM (2 mL) and TFA (5eq) was added at 4 °C. The mixture was stirred at room temperature for 2–5h, diluted in DCM (8 mL), washed three times with saturated $NaHCO_3$, once with brine, dried over Na_2SO_4, and the solvent was evaporated *in vacuo*. The crude residue was purified by flash column chromatography eluting with DCM/MeOH (100:0 to 95:5 or 90:10) to give desired derivatives **35–39**.

4.1.5.1. Methyl-[(3S)-3-phenyl-3-(4-((trifluoromethyanesulfonylphenoxy) propyl]-amine ***35***. ^{1}H RMN (400 MHz, $CDCl_3$) δ = 7.76 (d, *J* = 8.9 Hz, 2H), 7.30–7.18 (m, 5H), 6.98 (d, 2H), 5.37 (dd, *J* = 8.1, 4.8 Hz, 1H), 2.96 (bs, 1H), 2.79–2.62 (m, 2H), 2.39 (s, 3H), 2.27–2.17 (m, 1H), 2.11–1.97 (m, 1H). ^{13}C RMN (101 MHz, $CDCl_3$) δ 164.67, 139.73, 133.06, 129.08, 128.38, 125.74, 121.95, 119.85 (q, *J* = 325.5 Hz), 116.87, 79.10, 47.61, 37.86, 35.87. ^{19}F RMN (376 MHz, $CDCl_3$) δ −78.71. LC/MS (ESI): 374.12 $[M+H]^+$; HRMS (TOF, ESI+) cald for C17H18F3NO3S $[M+H]^+$ 374.103, found 374.1032; light yellow oil. Yield = 10 %.

4.1.5.2. 4-[(1S)-(3-(methylamino)-1-phenylpropoxy]benzonitrile ***36***. ^{1}H

RMN (400 MHz, $CDCl_3$) δ = 7.39 (d, *J* = 8.9 Hz, 2H), 7.28–7.20 (m, 5H), 6.82 (d, *J* = 8.9 Hz, 2H), 5.30 (dd, *J* = 8.1, 4.7 Hz, 1H), 2.82–2.70 (m, 2H), 2.41 (s, 3H), 2.27–2.16 (m, 1H), 2.12–2.00 (m, 1H). ^{13}C RMN (101 MHz, $CDCl_3$) δ = 161.17, 140.02, 133.87, 128.98, 128.21, 125.75, 119.12, 116.54, 104.13, 78.37, 47.53, 37.41, 35.49. LC/MS (ESI): 267.07 $[M+H]^+$; HRMS (TOF, ESI+) cald for C17H18N2O $[M+H]^+$ 267.149, found 267.1492; colorless oil. Yield = 25 %.

4.1.5.3. [(3S)-3-([1,1′-biphenyl]-4-yloxy)-3-phenylpropyl]-(methyl) amine ***37***. ^{1}H RMN (400 MHz, $CDCl_3$) δ 7.40 (d, *J* = 7.5 Hz, 2H), 7.34–7.27 (m, 6H), 7.25 (d, *J* = 7.6 Hz, 2H), 7.23–7.17 (m, 2H), 6.83 (d, *J* = 8.8 Hz, 2H), 5.26 (dd, *J* = 8.2, 4.3 Hz, 1H), 2.93–2.80 (m, 2H), 2.45 (s, 3H), 2.34–2.19 (m, 1H), 2.19–2.07 (m, 1H). ^{13}C RMN (101 MHz, $CDCl_3$) δ 157.33, 140.96, 140.69, 134.04, 128.81, 128.68, 128.06, 127.86, 126.69, 126.67, 125.87, 116.14, 77.90, 47.50, 36.92, 34.92. LC/MS (ESI): 318.26 $[M+H]^+$; HRMS (TOF, ESI+) cald for C22H23NO $[M+H]^+$ 318.185, found 318.1852; colorless oil. Yield = 22 %.

4.1.5.4. [(3S)-3-(4-benzylphenoxy)-3-phenylpropyl](methyl)amine ***38***. ^{1}H RMN (400 MHz, $CDCl_3$) δ 7.28–7.13 (m, 8H), 7.11–7.02 (m, 2H), 6.90 (d, *J* = 8.6 Hz, 2H), 6.67 (d, *J* = 8.6 Hz, 2H), 5.15 (dd, *J* = 8.3, 4.3 Hz, 1H), 3.77 (s, 2H), 2.92–2.77 (m 2H), 2.43 (s, 3H), 2.29–2.17 (m, 1H), 2.17–2.07 (m, 1H). ^{13}C RMN (101 MHz, $CDCl_3$) δ 156.10, 141.37, 140.96, 133.66, 129.73, 128.83, 128.76, 128.41, 127.81, 125.98, 125.83, 115.83, 77.72, 47.31, 41.01, 36.50, 34.53. LC/MS (ESI): 332.26 $[M+H]^+$; colorless oil. Yield = 8 %.

4.1.5.5. [(3S)-3-[4-fluoro-2-(trifluoromethyl)phenoxy]-3-phenylpropyl] (methyl)amine ***39***. ^{1}H RMN (400 MHz, $CDCl_3$) δ 7.31–7.18 (m, 6H), 7.08 (bd, *J* = 8.6 Hz, 1H), 6.78 (bt, *J* = 8.3 Hz, 1H), 5.31 (dd, *J* = 8.3, 4.7 Hz, 1H), 2.83–2.70 (m, 2H), 2.40 (s, 3H), 2.54 (bs, 1H), 2.30–2.18 (m1H), 2.09–1.97 (m1H). ^{13}C RMN (101 MHz, $CDCl_3$) δ 152.38 (d, $^1J_{CF}$ = 248.1 Hz), 148.74 (d, $^2J_{CF}$ = 10.2 Hz), 140.18, 128.91, 128.23, 125.84, 123.50 (qd, $^1J_{CF}$ = 271.5 Hz, $^4J_{CF}$ = 2.0 Hz), 123.33 (qd, 2JCF, 33.7 Hz, $^3J_{CF}$ = 6.8 Hz), 121.57 (m), 116.53 (d, $^3J_{CF}$ = 1.8 Hz), 113.69 (dq, $^2J_{CF}$ = 21.5 Hz, $^3J_{CF}$ = 3.6 Hz), 80.00, 47.81, 37.87, 35.91. ^{19}F RMN (376 MHz, $CDCl_3$) δ −61.88, −131.66. LC/MS (ESI): 328.20 $[M+H]^+$; HRMS (TOF, ESI+) cald for C17H17F4NO $[M+H]^+$ 328.132 found 328.1319; light yellow oil. Yield = 24 %.

4.1.6. General procedure for synthesis of derivatives ***41–49, 59, 63–69*** *and* ***80*** *via a Mitsunobu reaction*

To a stirred solution of triphenylphosphine (1.2 eq, 1.40 mmol) in dry THF (5 mL), cooled at 4 °C, was slowly added diisopropyl azodicarboxylate (DIAD, 1.2 eq, 1.40 mmol). After 30 min, the corresponding phenol (1.05 eq, 1.22 mmol) in dry THF (0.5 mL) was added and the reaction mixture was stirred 1h at 4 °C. Then, a solution of (*R*)-3-Chloro-1-phenylpropan-1-ol **40** (1 eq, 1.17 mmol) in dry THF (0.5 mL) was added at 4 °C. The reaction mixture was stirred at room temperature for 3–30h before removing the solvent *in vacuo*. The residue was diluted in DCM, washed twice with water, once with brine, dried over Na_2SO_4, and the solvent was evaporated *in vacuo*. The crude residue was purified by flash column chromatography eluting with cyclohexane/ethyl acetate (100:0 to 80:20) to give derivatives **41–49**, **59**, **63–69** and **80.**

4.1.6.1. 1-[(1S)-3-chloro-1-phenylpropoxy]-4-fluorobenzene ***41***. ^{1}H NMR (400 MHz, $CDCl_3$) δ 7.38–7.33 (m, 4H), 7.32–7.24 (m, 1H), 6.88 (dd, *J* = 9.2, 8.2 Hz, 2H), 6.80 (dd, *J* = 9.3, 4.5 Hz, 2H), 5.30 (dd, *J* = 8.6, 4.5 Hz, 1H), 3.82 (ddd, *J* = 10.9, 8.5, 5.3 Hz, 1H), 3.61 (dt, *J* = 11.1, 5.7 Hz, 1H), 2.46 (ddt, *J* = 14.2, 8.6, 5.5 Hz, 1H), 2.21 (dddd, *J* = 14.4, 8.5, 5.8, 4.5 Hz, 1H). ^{13}C NMR (101 MHz, $CDCl_3$) δ 157.40 (d, $^1J_{CF}$ = 239.0 Hz), 154.14 (d, $J\,^4_{CF}$ = 2.1 Hz), 140.75, 128.94, 128.13, 126.11, 117.33 (d, $J\,^3_{CF}$ = 8.0 Hz), 115.87 (d, $J\,^2_{CF}$ = 23.2 Hz), 77.82, 41.42. ^{19}F NMR (376 MHz, $CDCl_3$) δ −123.32. Light yellow oil. Yield = 27 %.

4.1.6.2. 1-chloro-4-[(1S)-3-chloro-1-phenylpropoxy]benzene ***42***. ^{1}H NMR (400 MHz, MeOD) δ 7.39–7.31 (m, 4H), 7.29–7.24 (m, 1H), 7.13 (d, *J* = 9.1 Hz, 2H), 6.84 (d, *J* = 9.1 Hz, 2H), 5.39 (dd, *J* = 8.7, 4.5 Hz, 1H), 3.78 (ddd, *J* = 10.9, 8.3, 5.9 Hz, 1H), 3.67–3.55 (m, 1H), 2.42 (ddt, *J* = 14.4, 8.7, 5.7 Hz, 1H), 2.19 (dddd, *J* = 14.5, 8.3, 6.4, 4.5 Hz, 1H). ^{13}C NMR (101 MHz, MeOD) δ 158.05, 141.92, 130.17, 129.83, 129.08, 127.20, 126.89, 118.58, 78.49, 42.51, 41.92. Light yellow oil. Yield = 35 %.

4.1.6.3. 1-bromo-4-[(1S)-3-chloro-1-phenylpropoxy]benzene ***43***. ^{1}H NMR (400 MHz, MeOD) δ 7.39–7.31 (m, 4H), 7.27 (d, *J* = 9.1 Hz, 2H), 7.29–7.24 (m, 1H), 6.79 (d, *J* = 9.1 Hz, 2H), 5.39 (dd, *J* = 8.7, 4.5 Hz, 1H), 3.78 (ddd, *J* = 11.0, 8.3, 5.9 Hz, 1H), 3.65–3.58 (m, 1H), 2.43 (ddt, *J* = 14.4, 8.7, 5.7 Hz, 1H), 2.19 (dddd, *J* = 14.5, 8.3, 6.4, 4.5 Hz, 1H). ^{13}C NMR (101 MHz, MeOD) δ 158.54, 141.87, 133.17, 129.84, 129.09, 127.19, 119.06, 114.06, 78.42, 42.50, 41.91. Light yellow oil. Yield = 65 %.

4.1.6.4. 1-[(1S)-3-chloro-1-phenylpropoxy]-4-iodobenzene ***44***. ^{1}H NMR (400 MHz, MeOD) δ 7.44 (d, *J* = 9.0 Hz, 2H), 7.38–7.31 (m, 4H), 7.29–7.23 (m, 1H), 6.67 (d, *J* = 9.0 Hz, 2H), 5.39 (dd, *J* = 8.7, 4.5 Hz, 1H), 3.76 (ddd, *J* = 11.0, 8.2, 5.9 Hz, 1H), 3.64–3.57 (m, 1H), 2.41 (ddt, *J* = 14.4, 8.7, 5.7 Hz, 1H), 2.18 (dddd, *J* = 14.5, 8.2, 6.4, 4.5 Hz, 1H). ^{13}C NMR (101 MHz, MeOD) δ 159.24, 141.83, 139.26, 129.83, 129.08, 127.16, 119.54, 83.70, 78.25, 42.48, 41.90. Light yellow oil. Yield = 33 %.

4.1.6.5. 1-[(1S)-3-chloro-1-phenylpropoxy]-4-methylbenzene ***45***. ^{1}H NMR (400 MHz, MeOD) δ 7.38–7.29 (m, 4H), 7.27–7.22 (m, 1H), 6.95 (dd, *J* = 8.8, 0.6 Hz, 2H), 6.73 (d, *J* = 8.6 Hz, 2H), 5.34 (dd, *J* = 8.7, 4.4 Hz, 1H), 3.78 (ddd, *J* = 10.9, 8.2, 5.9 Hz, 1H), 3.61 (ddd, *J* = 11.0, 6.3, 5.5 Hz, 1H), 2.40 (ddt, *J* = 14.4, 8.7, 5.7 Hz, 1H), 2.19 (s, 3H), 2.18–2.12 (m, 1H). ^{13}C NMR (101 MHz, MeOD) δ 157.23, 142.62, 131.35, 130.68, 129.68, 128.83, 127.20, 117.03, 78.21, 42.67, 42.07, 20.48. Light yellow oil. Yield = 70 %.

4.1.6.6. 1-Butyl-4-[(1S)-3-chloro-1-phenylpropoxy]benzene ***46***. ^{1}H NMR (400 MHz, $CDCl_3$) δ 7.41–7.33 (m, 4H), 7.31–7.25 (m, 1H), 7.01 (d, *J* = 8.7 Hz, 2H), 6.79 (d, *J* = 8.7 Hz, 2H), 5.34 (dd, *J* = 8.7, 4.4 Hz, 1H), 3.82 (ddd, *J* = 10.9, 8.3, 5.6 Hz, 1H), 3.70–3.57 (dt, *J* = 11.4, 5.7, 1H), 2.54–2.42 (m, 3H), 2.21 (dddd, *J* = 14.4, 8.3, 6.0, 4.4 Hz, 1H), 1.53 (m, 2H), 1.33 (m, 2H), 0.91 (t, *J* = 7.3 Hz, 3H). ^{13}C NMR (101 MHz, $CDCl_3$) δ 156.11, 141.30, 135.54, 129.30, 128.86, 127.90, 126.06, 115.88, 77.01, 41.66, 41.52, 34.83, 33.91, 22.44, 14.07. Light yellow oil. Yield = 34 %.

4.1.6.7. 1-[(1S)-3-chloro-1-phenylpropoxy]-4-methoxybenzene ***47***. ^{1}H NMR (400 MHz, $CDCl_3$) δ 7.41–7.32 (m, 4H), 7.31–7.25 (m, 1H), 6.81 (d, *J* = 9.2 Hz, 2H), 6.74 (d, *J* = 9.2 Hz, 2H), 5.28 (dd, *J* = 8.7, 4.4 Hz, 1H), 3.83 (ddd, *J* = 10.9, 8.4, 5.5 Hz, 1H), 3.72 (s, 3H), 3.63 (dt, *J* = 11.1, 5.7 Hz, 1H), 2.46 (ddt, *J* = 14.3, 8.7, 5.5 Hz, 1H), 2.21 (dddd, *J* = 14.4, 8.4, 5.9, 4.5 Hz, 1H). ^{13}C NMR (101 MHz, $CDCl_3$) δ 154.15, 152.17, 141.23, 128.83, 127.94, 126.16, 117.32, 114.63, 77.87, 55.72, 41.53, 41.49. Yellow oil. Yield = 18 %.

4.1.6.8. 1-[(1S)-3-chloro-1-phenylpropoxy]-4-propoxybenzene ***48***. ^{1}H NMR (400 MHz, $CDCl_3$) δ 7.39–7.31 (m, 4H), 7.29–7.23 (m, 1H), 6.77 (d, *J* = 9.3 Hz, 2H), 6.72 (d, *J* = 9.2 Hz, 2H), 5.25 (dd, *J* = 8.7, 4.4 Hz, 1H), 3.86–3.78 (m, 1H), 3.81 (t, *J* = 6.6 Hz, 2H), 3.61 (dt, *J* = 11.2, 5.8 Hz, 1H), 2.44 (ddt, *J* = 14.3, 8.7, 5.5 Hz, 1H), 2.19 (dddd, *J* = 14.4, 8.4, 5.9, 4.5 Hz, 1H), 1.79–1.67 (m, 2H), 0.99 (t, *J* = 7.4 Hz, 3H). ^{13}C NMR (101 MHz, $CDCl_3$) δ 153.73, 152.07, 141.29, 128.83, 127.94, 126.19, 117.32, 115.37, 77.90, 70.13, 41.56, 41.53, 22.77, 10.64. Yellow oil. Yield = 18 %.

4.1.6.9. 1-[(1S)-3-chloro-1-phenylpropoxy]-4-(trifluoromethoxy)benzene ***49***. ^{1}H NMR (400 MHz, MeOD) δ 7.40–7.32 (m, 4H), 7.29–7.24 (m, 1H), 7.07 (dd, J = 9.2, 0.8 Hz, 2H), 6.91 (d, J = 9.2 Hz, 2H), 5.42 (dd, J = 8.7, 4.5 Hz, 1H), 3.78 (ddd, J = 11.0, 8.3, 5.9 Hz, 1H), 3.66–3.58 (m, 1H), 2.44 (ddt, J = 14.4, 8.7, 5.7 Hz, 1H), 2.20 (dddd, J = 14.5, 8.3, 6.4, 4.5 Hz, 1H). ^{13}C NMR (101 MHz, MeOD) δ 158.04, 144.10 (q, $^{3}J_{CF}$ = 1.9 Hz), 141.83, 129.87, 129.13, 127.19, 123.30, 121.95 (q, $^{1}J_{CF}$ = 254.5 Hz), 118.06, 78.62, 42.51, 41.89. ^{19}F NMR (376 MHz, MeOD) δ −59.97. Colorless oil. Yield = 44 %.

4.1.6.10. 1-{[(1S)-3-chloro-1-phenylpropyl]sulfanyl}-4-(trifluoromethyl) benzene ***59***. ^{1}H NMR (400 MHz, MeOD) δ 7.50 (d, J = 8.3 Hz, 2H), 7.43 (d, J = 8.2 Hz, 2H), 7.38–7.28 (m, 4H), 7.27–7.22 (m, 1H), 4.65 (dd, J = 8.5, 6.6 Hz, 1H), 3.64 (dt, J = 11.2, 6.0 Hz, 1H), 3.42 (ddd, J = 11.1, 7.7, 6.0 Hz, 1H), 2.47–2.28 (m, 2H). ^{13}C NMR (101 MHz, MeOD) δ 141.95, 141.60, 131.81, 129.78, 129.53 (q, $^{2}J_{CF}$ = 32.4 Hz), 128.99, 128.87, 126.56 (q, $^{3}J_{CF}$ = 3.7 Hz), 125.58 (q, $^{1}J_{CF}$ = 270.8 Hz), 50.27, 43.02, 40.02. ^{19}F NMR (376 MHz, MeOD) δ −64.09. Colorless oil. Yield = 67 %

4.1.6.11. 2-[(1S)-3-chloro-1-phenylpropoxy]naphthalene ***63***. ^{1}H NMR (400 MHz, $CDCl_3$) δ 7.72 (d, J = 8.1 Hz, 1H), 7.71 (d, J = 9.0 Hz, 1H), 7.59 (d, J = 8.2 Hz, 1H), 7.46–7.42 (m, 2H), 7.39–7.29 (m, 4H), 7.29–7.24 (m, 1H), 7.19 (dd, J = 8.9, 2.5 Hz, 1H), 7.05 (d, J = 2.5 Hz, 1H), 5.54 (dd, J = 8.5, 4.5 Hz, 1H), 3.85 (ddd, J = 11.0, 8.3, 5.5 Hz, 1H), 3.70–3.59 (m, 1H), 2.53 (ddt, J = 14.2, 8.5, 5.6 Hz, 1H), 2.28 (dddd, J = 14.4, 8.3, 5.9, 4.5 Hz, 1H).^{13}C NMR (101 MHz, $CDCl_3$) δ 155.83, 140.84, 134.46, 129.52, 129.17, 128.96, 128.06, 127.68, 126.99, 126.38, 126.08, 123.88, 119.30, 109.60, 76.98, 41.54, 41.48. White solid. Yield = 34 %.

4.1.6.12. 1-[(1S)-3-chloro-1-phenylpropoxy]-2-methoxy-4-(prop-2-ene-1-yl)benzene ***64***. ^{1}H NMR (400 MHz, $CDCl_3$): δ 7.42–7.31 (m, 4H); 7.30–7.24 (m, 1H); 6.70 (d, J = 2.0 Hz, 1H); 6.65 (d, J = 8.2 Hz, 1H); 6.54 (dd, J = 8.2, 2.0 Hz, 1H); 5.91 (ddt, J = 16.9, 10.1, 6.7 Hz, 1H); 5.30 (dd, J = 8.8, 4.3 Hz, 1H); 5.08–5.01 (m, 2H); 3.90 (m, 1H); 3.87 (s, 1H); 3.65 (dt, J = 11.1, 5.7, 1H); 3.28 (d, J = 6.7, 2H); 2.55 (ddt, J = 14.4, 8.8, 5.5 Hz, 1H); 2.20 (dddd, J = 14.5, 8.4, 5.9, 4.3 Hz, 1H**).** ^{13}C NMR (101 MHz, $CDCl_3$) δ 150.18, 145.92, 141.33, 137.66, 133.84, 128.75, 127.93, 126.22, 120.51, 116.70, 115.78, 112.63, 78.84, 56.06, 41.77, 41.55, 39.95. Yellow oil. Yield = 17 %.

4.1.6.13. 5-Bromo-2-[(1S)-3-chloro-1-phenylpropoxy]benzonitrile ***65***. ^{1}H NMR (400 MHz, $CDCl_3$) δ 7.63 (d, J = 2.5 Hz, 1H), 7.43 (dd, J = 9.0, 2.5 Hz, 1H), 7.39–7.34 (m, 4H), 7.33–7.29 (m, 1H), 6.71 (d, J = 9.1 Hz, 1H), 5.48 (dd, J = 8.8, 4.4 Hz, 1H), 3.88 (ddd, J = 11.2, 9.2, 4.4 Hz, 1H), 3.63 (dt, J = 10.9, 5.3 Hz, 1H), 2.57 (dddd, J = 14.4, 8.8, 5.4, 4.4 Hz, 1H), 2.30–2.19 (m, 1H). ^{13}C NMR (101 MHz, $CDCl_3$) δ 158.82, 139.03, 137.17, 135.91, 129.30, 128.78, 125.96, 116.10, 115.08, 112.92, 104.67, 78.53, 41.16, 40.97. Light yellow oil. Yield = 44 %.

4.1.6.14. 1-Chloro-4-[(1S)-3-chloro-1-phenylpropoxy]-2-methylbenzene ***66***. ^{1}H NMR (400 MHz, $CDCl_3$): δ 7.34–7.29 (m, 4H); 7.26–7.21 (m, 1H); 7.08 (d, J = 8.7 Hz, 1H); 6.74 (d, J = 2.9 Hz, 1H); 6.58 (dd, J = 8.7, 3.0 Hz, 1H), 5.30 (dd, J = 8.6, 4.5 Hz, 1H); 3.75 (ddd, J = 10.9, 8.5, 5.3 Hz, 1H); 3.56 (dt, J = 11.1, 5.7 Hz, 1H), 2.41 (ddt, J = 14.2, 8.6, 5.5 Hz, 1H); 2.23 (s, 3H); 2,17 (dddd, J = 14.4, 8.5, 5.8, 4.5 Hz, 1H). ^{13}C NMR (101 MHz, $CDCl_3$) δ 156.55, 140.67, 137.10, 129.64, 128.96, 128.13, 126.35, 126.02, 118.83, 114.56, 77.09, 41.43, 41.37, 20.42. Colorless oil. Yield = 20 %.

4.1.6.15. 1-[(1S)-3-chloro-1-phenylpropoxy]-2-methyl-3-nitrobenzene ***67***. ^{1}H NMR (400 MHz, MeOD) δ 7.41–7.33 (m, 4H), 7.31–7.25 (m, 2H), 7.15 (bt, J = 8.3 Hz, 1H), 7.01 (bd, J = 8.2 Hz, 1H), 5.56 (dd, J = 8.5, 4.6 Hz, 1H), 3.81 (ddd, J = 11.0, 8.2, 5.8 Hz, 1H), 3.71–3.60 (m, 1H), 2.54 (ddt, J = 14.3, 8.5, 5.7 Hz, 1H), 2.41 (s, 3H), 2.27 (dddd, J = 14.5, 8.2, 6.3, 4.6 Hz, 1H). ^{13}C NMR (101 MHz, MeOD) δ 160.19, 151.29, 141.31, 129.98, 129.34, 127.81, 127.17, 122.86, 118.14, 116.85, 79.02, 42.28, 41.91, 11.87. Yellow oil. Yield = 42 %.

4.1.6.16. 4-Chloro-1-[(1S)-3-chloro-1-phenylpropoxy]-2-nitrobenzene ***68***. ^{1}H NMR (400 MHz, MeOD) δ 7.82 (d, J = 2.6 Hz, 1H), 7.43–7.34 (m, 4H), 7.33–7.28 (m, 1H), 7.06 (d, J = 9.1 Hz, 1H), 5.65 (dd, J = 8.8, 4.3 Hz, 1H), 3.81 (ddd, J = 11.0, 8.5, 5.7 Hz, 1H), 3.64 (ddd, J = 11.2, 6.2, 5.4 Hz, 1H), 2.48 (ddt, J = 14.4, 8.8, 5.5 Hz, 1H), 2.24 (dddd, J = 14.7, 8.5, 6.3, 4.4 Hz, 1H). ^{13}C NMR (101 MHz, MeOD) δ 150.58, 142.14, 140.51, 134.41, 130.10, 129.62, 127.20, 126.49, 125.90, 118.95, 79.96, 42.17, 41.62. Light orange oil. Yield = 45 %.

4.1.6.17. 4-[(1S)-3-chloro-1-phenylpropoxy]-2-nitrobenzonitrile ***69***. ^{1}H NMR (400 MHz, MeOD) δ 7.86 (d, J = 2.6 Hz, 1H), 7.82 (d, J = 8.7 Hz, 1H), 7.45 (m, 1H), 7.41–7.36 (m, 4H), 7.34–7.28 (m, 1H), 5.69 (dd, J = 8.5, 4.7 Hz, 1H), 3.79 (ddd, J = 11.1, 8.2, 5.8 Hz, 1H), 3.68–3.59 (m, 1H), 2.55 (ddt, J = 14.3, 8.5, 5.7 Hz, 1H), 2.29 (dddd, J = 14.5, 8.2, 6.3, 4.7 Hz, 1H). ^{13}C NMR (101 MHz, MeOD) δ 162.99, 151.44, 140.14, 137.98, 130.21, 129.77, 127.32, 122.34, 116.32, 114.45, 100.29, 79.80, 41.98, 41.56. Yellow oil. Yield = 55 %.

4.1.6.18. 1-[(1S)-3-chloro-1-phenylpropoxy]-4-iodobenzene ***80***. ^{1}H NMR (400 MHz, MeOD) δ 7.44 (d, J = 9.0 Hz, 2H), 7.38–7.30 (m, 4H), 7.29–7.23 (m, 1H), 6.67 (d, J = 9.0 Hz, 2H), 5.38 (dd, J = 8.6, 4.5 Hz, 1H), 3.76 (ddd, J = 10.9, 8.2, 5.9 Hz, 1H), 3.60 (ddd, J = 10.9, 6.4, 5.4 Hz, 1H), 2.41 (ddt, J = 14.5, 8.7, 5.7 Hz, 1H), 2.18 (dddd, J = 14.5, 8.2, 6.4, 4.5 Hz, 1H). ^{13}C NMR (101 MHz, MeOD) δ 159.21, 141.81, 139.25, 129.83, 129.08, 127.15, 119.52, 83.70, 78.20, 42.47, 41.91. Yellow oil, 43 %

4.1.7. General procedure for synthesis of derivatives ***50–58***, ***60*** *and* ***70–76*** *via a methylamination reaction*

To a stirred solution of (1*S*)-(3-chloro-1-phenylpropoxy)benzene derivatives **41–49**, **59** and **63–69** (1 eq) in EtOH (4 mL) was added a solution methylamine (40 % in water, 30 eq). The reaction mixture was heated at 120 °C for 1h before removing the solvent *in vacuo*. The residue was diluted in DCM, the organic phase was washed twice with water, once with brine, dried over Na2SO4, and concentrated under vacuum. The crude residue was purified by flash column chromatography as indicated for each compound to give derivatives **50–58**, **60** and **70–76**.

4.1.7.1. [(3S)-3-(4-fluorophenoxy)-3-phenylpropyl](methyl)amine ***50***. Chromatography on silica gel was eluting with DCM to DCM/MeOH 85/15 (v/v). ^{1}H NMR (400 MHz, MeOD) δ 7.40–7.31 (m, 4H), 7.29–7.24 (m, 1H), 6.92–6.82 (m, 4H), 5.29 (dd, J = 8.3, 4.4 Hz, 1H), 3.05–2.90 (m, 2H), 2.55 (s, 3H), 2.25 (ddt, J = 14.2, 8.7, 5.9 Hz, 1H), 2.11 (dddd, J = 13.7, 9.1, 6.0, 4.4 Hz, 1H). ^{13}C NMR (101 MHz, MeOD) δ 158.93 (d, $^{1}J_{CF}$ = 237.7 Hz), 155.38 (d, J^{4}_{CF} = 2.0 Hz), 142.17, 129.96, 129.22, 127.33, 118.42 (d, J^{3}_{CF} = 8.1 Hz), 116.53 (d, J^{2}_{CF} = 23.5 Hz), 79.73, 49.43, 37.48, 34.91. ^{19}F NMR (376 MHz, MEOD) δ −125.59. LC/MS (ESI): 260.37 $[M+H]^+$; HRMS (TOF, ESI+) cald for $C_{16}H_{18}FNO$ $[M+H]^+$ 260.144, found 260.1445; Light yellow oil. Yield = 62 %.

4.1.7.2. [(3S)-3-(4-chlorophenoxy)-methyl-phenylpropyl](methyl)amine ***51***. Chromatography on silica gel was eluting with DCM to DCM/MeOH 90/10 (v/v). ^{1}H NMR (400 MHz, MeOD) δ 7.38–7.30 (m, 4H), 7.28–7.22 (m, 1H), 7.13 (d, J = 9.1 Hz, 2H), 6.83 (d, J = 9.1 Hz, 2H), 5.28 (dd, J = 8.1, 4.8 Hz, 1H), 2.71 (m, 2H), 2.37 (s, 3H), 2.17 (dtd, J = 14.0, 8.3, 5.8 Hz, 1H), 2.02 (dddd, J = 13.7, 8.7, 6.3, 4.8 Hz, 1H). ^{13}C NMR (101 MHz, MeOD) δ 158.07, 142.63, 130.11, 129.71, 128.85, 127.14, 126.66, 118.53, 79.80, 49.07, 39.00, 36.01. LC/MS (ESI): 276.61 $[M+H]^+$; HRMS (TOF, ESI+) cald for C16H18ClNO $[M+H]^+$ 276.115, found

276.115; Light yellow oil. Yield = 58 %.

4.1.7.3. [(3S)-3-(4-bromophenoxy)-3-phenylpropyl](methyl)amine ***52***. Chromatography on silica gel was eluting with DCM to DCM/MeOH 90/10 (v/v). ^{1}H NMR (400 MHz, MeOD) δ 7.37–7.29 (m, 4H), 7.26 (d, J = 9.1 Hz, 2H), 7.25–7.21 (m, 1H), 6.78 (d, J = 9.1 Hz, 2H), 5.28 (dd, J = 8.1, 4.8 Hz, 1H), 2.79–2.62 (m, 2H), 2.36 (s, 3H), 2.17 (dtd, J = 14.0, 8.3, 5.8 Hz, 1H), 2.01 (dddd, J = 13.7, 8.7, 6.3, 4.8 Hz, 1H). ^{13}C NMR (101 MHz, MeOD) δ 158.57, 142.61, 133.11, 129.71, 128.85, 127.13, 119.02, 113.80, 79.75, 49.28, 39.07, 36.06. LC/MS (ESI): 320.54 and 322.54 $[M+H]^+$; HRMS (TOF, ESI+) cald for C16H18BrNO $[M+H]^+$ 320.064, found 320.0645 and 322.0626; Yellow oil. Yield = 46 %.

4.1.7.4. [(3S)-3-(4-iodophenoxy)-3-phenylpropyl](methyl)amine ***53***. Chromatography on silica gel was eluting with DCM to DCM/MeOH 95/5 (v/v). ^{1}H NMR (400 MHz, MeOD) δ 7.44 (d, J = 9.0 Hz, 2H), 7.37–7.29 (m, 4H), 7.27–7.21 (m, 1H), 6.67 (d, J = 9.0 Hz, 2H), 5.28 (dd, J = 8.1, 4.8 Hz, 1H), 2.71 (m,2H), 2.37 (s, 3H), 2.17 (dtd, J = 14.0, 8.2, 6.0 Hz, 1H), 2.07–1.96 (m, 1H). ^{13}C NMR (101 MHz, MeOD) δ 159.28, 142.55, 139.21, 129.72, 128.85, 127.11, 119.53, 83.42, 79.57, 48.97, 38.97, 36.00. LC/MS (ESI): 368.41 $[M+H]^+$; HRMS (TOF, ESI+) cald for $C_{16}H_{18}INO$ $[M+H]^+$ 368.050, found 368.0506; Chiral analytical analysis, method 2: RT, 7.56 min, 95 % ee; Light yellow oil. Yield = 59 %.

4.1.7.5. Methyl [(3S)-3-(4-methylphenoxy)-3-phenylpropyl]amine ***54***. Chromatography on silica gel was eluting with DCM to DCM/MeOH 95/5 (v/v). ^{1}H NMR (400 MHz, MeOD) δ 7.38–7.27 (m, 4H), 7.25–7.19 (m, 1H), 6.94 (d, J = 8.7 Hz, 2H), 6.72 (d, J = 8.6 Hz, 2H), 5.24 (dd, J = 8.1, 4.7 Hz, 1H), 2.79–2.63 (m, 2H), 2.36 (s, 3H), 2.18 (s, 3H), 2.17–2.09 (m, 1H), 2.00 (dddd, J = 13.7, 8.7, 6.3, 4.8 Hz, 1H). ^{13}C NMR (101 MHz, MeOD) δ 155.83, 141.90, 129.73, 129.25, 128.17, 127.20, 125.75, 115.55, 78.19, 47.77, 37.68, 34.62, 19.07. LC/MS (ESI): 256.56 $[M+H]^+$; HRMS (TOF, ESI+) cald for $C_{17}H_{21}NO$ $[M+H]^+$ 256.169, found 256.1696; Light yellow oil. Yield = 43 %.

4.1.7.6. [(3S)-3-(4-butylphenoxy)-3-phenylpropyl](methyl)amine ***55***. Chromatography on silica gel was eluting with DCM to DCM/MeOH 85/15 (v/v). ^{1}H NMR (400 MHz, MeOD) δ 7.42–7.32 (m, 4H), 7.30–7.25 (m, 1H), 6.98 (d, J = 8.7 Hz, 2H), 6.78 (d, J = 8.7 Hz, 2H), 5.35 (dd, J = 8.4, 4.1 Hz, 1H), 3.18 (m, 2H), 2.70 (s, 3H), 2.48 (t, J = 7.6 Hz, 2H), 2.37–2.13 (m, 2H), 1.50 (m, 2H), 1.29 (m, 2H), 0.89 (t, J = 7.3 Hz, 3H). ^{13}C NMR (101 MHz, MeOD) δ 156.86, 142.08, 136.85, 130.16, 129.83, 129.08, 127.08, 116.96, 78.65, 47.81, 36.26, 35.65, 35.08, 34.02, 23.23, 14.23. LC/MS (ESI): 298.43 $[M+H]^+$; HRMS (TOF, ESI+) cald for $C_{20}H_{27}NO$ $[M+H]^+$ 298.2165, found 298.2165; Colorless oil. Yield = 24 %.

4.1.7.7. [(3S)-3-(4-methoxyphenoxy)-3-phenylpropyl](methyl)amine ***56***. Chromatography on silica gel was eluting with DCM to DCM/MeOH 85/15 (v/v). ^{1}H NMR (400 MHz, MeOD) δ 7.42–7.31 (m, 4H), 7.30–7.24 (m, 1H), 6.81 (d, J = 9.3 Hz, 2H), 6.73 (d, J = 9.3 Hz, 2H), 5.30 (dd, J = 8.4, 4.1 Hz, 1H), 3.67 (s, 3H), 3.29–3.21 (m, 1H), 3.20–3.12 (m, 1H), 2.72 (s, 3H), 2.37–2.27 (m, 1H), 2.21 (m, 1H). ^{13}C NMR (101 MHz, MeOD) δ 155.76, 152.76, 142.00, 129.81, 129.13, 127.22, 118.32, 115.49, 79.38, 56.01, 47.78, 36.03, 33.92. LC/MS (ESI): 272.43 $[M+H]^+$; HRMS (TOF, ESI+) cald for $C_{17}H_{21}NO_2$ $[M+H]^+$ 272.164, found 272.1645; Colorless oil. Yield = 21 %.

4.1.7.8. Methyl[(3S)-3-phenyl-3-(4-propoxyphenoxy)propyl]amine ***57***. Chromatography on silica gel was eluting with DCM to DCM/MeOH 95/5 (v/v). ^{1}H NMR (400 MHz, MeOD) δ 7.42–7.31 (m, 4H), 7.30–7.24 (m, 1H), 6.79 (d, J = 9.3 Hz, 2H), 6.72 (d, J = 9.3 Hz, 2H), 5.29 (dd, J = 8.4, 4.1 Hz, 1H), 3.80 (t, J = 6.5 Hz, 2H), 3.21 (m, 2H), 2.72 (s, 3H), 2.36–2.26 (m, 1H), 2.26–2.15 (m, 1H), 1.76–1.64 (m, 2H), 0.99 (t, J = 7.4 Hz, 3H). ^{13}C NMR (101 MHz, MeOD) δ 155.20, 152.72, 142.02, 129.81, 129.13, 127.21, 118.29, 116.24, 79.38, 71.05, 47.78, 36.03, 33.91, 23.69, 10.80. LC/MS (ESI): 300.45 $[M+H]^+$; HRMS (TOF, ESI+) cald for $C_{19}H_{25}NO_2$ $[M+H]^+$ 300.196, found 300.1958; Colorless oil. Yield = 16 %.

4.1.7.9. Methyl-[(3S)-3-phenyl-3-(4-(trifluoromethoxy)phenoxy)propyl]-amine ***58***. Chromatography on silica gel was eluting with DCM to DCM/MeOH 90/10 (v/v). ^{1}H NMR (400 MHz, MeOD) δ 7.40–7.31 (m, 4H), 7.28–7.23 (m, 1H), 7.07 (dd, J = 9.2, 0.8 Hz, 2H), 6.91 (d, J = 9.2 Hz, 2H), 5.32 (dd, J = 8.1, 4.7 Hz, 1H), 2.76 (m, 2H), 2.40 (s, 3H), 2.20 (dtd, J = 14.0, 8.3, 5.9 Hz, 1H), 2.05 (dddd, J = 13.7, 8.7, 6.3, 4.7 Hz, 1H). ^{13}C NMR (101 MHz, MeOD) δ 158.05, 143.99 (q, $^{3}J_{CF}$ = 2.0 Hz), 142.45, 129.78, 128.94, 127.14, 123.28, 121.97 (q, $^{1}J_{CF}$ = 254.3 Hz), 118.03, 79.85, 48.86, 38.77, 35.84. ^{19}F NMR (376 MHz, MeOD) δ 60.04. LC/MS (ESI): 326.58 $[M+H]^+$; HRMS (TOF, ESI+) cald for C17H18F3NO $[M+H]^+$ 326.136, found 326.1362; Light yellow oil. Yield = 76 %.

4.1.7.10. Methyl[(3S)-3-phenyl-3-{[4-(trifluoromethyl)phenyl]sulfanyl} propyl]amine ***60***. Chromatography on silica gel was eluting with DCM to DCM/MeOH 92/8 (v/v). ^{1}H NMR (400 MHz, MeOD) δ 7.48 (d, J = 8.4 Hz, 2H), 7.42 (d, J = 8.3 Hz, 2H), 7.38–7.26 (m, 4H), 7.25–7.19 (m, 1H), 4.52 (dd, J = 8.6, 6.5 Hz, 1H), 2.66 (ddd, J = 11.9, 9.0, 6.2 Hz, 1H), 2.56 (ddd, J = 11.9, 8.8, 5.9 Hz, 1H), 2.35 (s, 3H), 2.25–2.08 (m, 2H).^{13}C NMR (101 MHz, MeOD) δ 142.42, 142.25, 131.78, 129.67, 129.36 (q, $^{2}J_{CF}$ = 32.6 Hz), 128.88, 128.67, 126.46 (q, $^{3}J_{CF}$ = 3.9 Hz), 125.66 (q, $^{1}J_{CF}$ = 541.5, 270.5 Hz), 50.89, 50.08, 36.56, 35.70. ^{19}F NMR (376 MHz, MeOD) δ −64.10. LC/MS (ESI): 326.28 $[M+H]^+$; HRMS (TOF, ESI+) cald for C17H18F3NS $[M+H]^+$ 326.118, found 326.1185; Yellow oil. Yield = 16 %

4.1.7.11. Methyl[(3S)-3-(naphtalen-2-yloxy)-3-phenylpropyl]amine ***70***. Chromatography on silica gel was eluting with DCM to DCM/MeOH 90/10 (v/v). ^{1}H RMN (400 MHz, $CDCl_3$) δ 7.72 (d, J = 7.9 Hz, 1H), 7.70 (d, J = 8.9 Hz, 1H), 7.57 (d, J = 8.1 Hz, 1H), 7.43–7.40 (m, 2H), 7.38–7.28 (m, 4H), 7.27–7.22 (m, 1H), 7.19 (dd, J = 8.9, 2.5 Hz, 1H), 7.03 (d, J = 2.4 Hz, 1H), 5.41 (dd, J = 8.2, 4.6 Hz, 1H), 3.08 (bs, 1H), 2.85 (t, J = 6.9 Hz, 2H), 2.47 (s3H), 2.36–2.21 (m, 1H), 2.18–2.06 (m, 1H). ^{13}C RMN (101 MHz, $CDCl_3$) δ 155.80, 141.41, 134.36, 129.35, 128.95, 128.72, 127.69, 127.54, 126.82, 126.21, 125.90, 123.66, 119.25, 109.31, 78.27, 48.08, 38.08, 35.91. LC/MS (ESI): 292.30 $[M+H]^+$; HRMS (TOF, ESI+) cald for $C_{20}H_{21}NO$ $[M+H]^+$ 292.1698, found 292.1696; colorless oil. Yield = 52 %.

4.1.7.12. [(3S)-3-[2-methoxy-4-(prop-2-en-1-yl)phenoxy]-3-phenyl-propyl](methyl)amine ***71***. Chromatography on silica gel was eluting with DCM to DCM/MeOH 95/5 (v/v). ^{1}H NMR (400 MHz, MeOD) δ 7.41–7.34 (m, 4H), 7.33–7.28 (m, 1H), 6.85–6.82 (bs, 1H), 6.51 (m, 2H), 5.90 (ddt, J = 16.8, 10.1, 6.7 Hz, 1H), 5.25 (dd, J = 9.3, 3.6 Hz, 1H), 5.05–4.97 (m, 2H), 3.92 (s, 3H), 3.37 (ddd, J = 12.9, 8.2, 5.8 Hz, 1H), 3.30–3.22 (m, 3H), 2.80 (s, 3H), 2.41–2.28 (m, 1H), 2.26–2.14 (m, 1H). ^{13}C NMR (101 MHz, MeOD) δ 151.19, 146.10, 141.99, 138.90, 136.19, 129.82, 129.32, 127.21, 121.54, 118.39, 115.85, 113.38, 82.71, 56.49, 49.05, 40.72, 35.66, 33.95. LC/MS (ESI): 312.44 $[M+H]^+$; HRMS (TOF, ESI+) cald for $C_{20}H_{25}NO_2$ $[M+H]^+$ 312.196, found 312.1958; Yellow oil. Yield = 16 %.

4.1.7.13. 5-Bromo-2-[(1S)-3-(methylamino)-1-phenylpropoxy]benzonitrile ***72***. Chromatography on silica gel was eluting with DCM to DCM/MeOH 95/5 (v/v). ^{1}H NMR (400 MHz, MeOD) δ 7.76 (d, J = 2.5 Hz, 1H), 7.54 (dd, J = 9.1, 2.5 Hz, 1H), 7.41–7.34 (m, 4H), 7.32–7.26 (m, 1H), 6.90 (d, J = 9.1 Hz, 1H), 5.52 (dd, J = 8.1, 4.8 Hz, 1H), 2.83–2.68 (m, 2H), 2.39 (s, 3H), 2.27 (m, 1H), 2.10 (dddd, J = 14.0, 8.2, 6.7, 4.8 Hz, 1H). ^{13}C NMR (101 MHz, MeOD) δ 160.28, 141.26, 138.32, 136.76, 130.00, 129.40, 127.10, 117.84, 116.02, 113.54, 105.37, 81.27, 48.69, 38.64, 36.01. LC/MS (ESI): 347.26 $[M+H]^+$; HRMS (TOF, ESI+) cald for

$C_{17}H_{17}BrN_2O$ $[M+H]^+$ 345.059, found 345.0597; Colorless oil. Yield = 38 %.

*4.1.7.14. [(3S)-3-(4-chloro-3-methylphenoxy)-3-phenylpropyl](methyl) amine **73**.* Chromatography on silica gel was eluting with DCM to DCM/MeOH 95/5 (v/v). ^{1}H NMR (400 MHz, MeOD) δ 7.38–7.30 (m, 4H), 7.27–7.22 (m, 1H), 7.09 (d, *J* = 8.8 Hz, 1H), 6.80 (d, *J* = 2.7 Hz, 1H), 6.65 (dd, *J* = 8.8, 2.8 Hz, 1H), 5.28 (dd, *J* = 8.1, 4.8 Hz, 1H), 2.70 (m, 2H), 2.37 (s, 3H), 2.23 (s, 3H), 2.21–2.10 (m, 1H), 2.00 (dddd, *J* = 13.7, 8.7, 6.3, 4.8 Hz, 1H). ^{13}C NMR (101 MHz, MeOD) δ 158.03, 142.79, 137.85, 130.39, 129.68, 128.79, 127.13, 126.79, 119.69, 115.87, 79.68, 49.04, 39.04, 36.04, 20.22. LC/MS (ESI): 290.37 $[M+H]^+$; HRMS (TOF, ESI+) cald for $C_{17}H_{20}$Cl NO $[M+H]^+$ 290.130, found 290.1306; Colorless oil. Yield = 70 %.

*4.1.7.15. Methyl[(3S)-3-(2-methyl-3-nitrophenoxy)-3-phenylpropyl] amine **74**.* Chromatography on silica gel was eluting with DCM to DCM/MeOH 90/10 (v/v). ^{1}H NMR (400 MHz, MeOD) δ 7.39–7.31 (m, 4H), 7.29–7.23 (m, 2H), 7.10 (bt, *J* = 8.3 Hz, 1H), 7.00 (bd, *J* = 8.3 Hz, 1H), 5.45 (dd, *J* = 8.0, 4.9 Hz, 1H), 2.83–2.65 (m, 2H), 2.41 (s, 3H), 2.38 (s, 3H), 2.33–2.19 (m, 1H), 2.15–2.04 (m, 1H). ^{13}C NMR (101 MHz, MeOD) δ 157.80, 152.65, 142.06, 129.86, 129.09, 127.74, 127.07, 122.75, 118.22, 116.65, 80.23, 48.94, 38.92, 36.03, 11.90. LC/MS (ESI): 301.59 $[M+H]^+$;HRMS (TOF, ESI+) cald for $C_{17}H_{20}N_2O_3$ $[M+H]^+$ 301.1549 found 301.1547 Colorless oil. Yield = 40 %.

*4.1.7.16. [(3S)-3-(4-chloro-2-nitrophenoxy)-3-phenylpropyl](methyl) amine **75**.* Chromatography on silica gel was eluting with DCM to DCM/MeOH 80/20 (v/v). ^{1}H NMR (400 MHz, MeOD) δ 7.89 (d, *J* = 2.6 Hz, 1H), 7.44–7.36 (m, 4H), 7.35–7.30 (m, 1H), 7.04 (d, *J* = 9.1 Hz, 1H), 5.66 (dd, *J* = 8.4, 4.1 Hz, 1H), 3.22–3.05 (m, 2H), 2.67 (s, 3H), 2.41–2.29 (m, 1H), 2.28–2.21 (m, 1H). ^{13}C NMR (101 MHz, MeOD) δ 150.60, 142.12, 141.12, 134.35, 130.00, 129.40, 127.10, 126.33, 125.84, 119.11, 81.40, 48.61, 38.45, 35.87. LC/MS (ESI): 321.34 $[M+H]^+$; HRMS (TOF, ESI+) cald for C16H17ClN2O3 $[M+H]^+$ 321.099, found 321.1; Colorless oil. Yield = 20 %.

*4.1.7.17. 4-[(1S)-3-(methylamino)-1-phenylpropoxy]-2-nitrobenzonitrile **76**.* Chromatography on silica gel was eluting with DCM to DCM/MeOH 90/10 (v/v). ^{1}H NMR (400 MHz, MeOD) δ 7.84 (d, *J* = 2.6 Hz, 1H), 7.81 (d, *J* = 8.7 Hz, 1H), 7.44–7.41 (m, 2H), 7.40–7.34 (m, 4H), 7.32–7.27 (m, 1H), 5.59 (dd, *J* = 8.1, 4.9 Hz, 1H), 2.82–2.66 (m, 2H), 2.40 (s, 3H), 2.29 (dtd, *J* = 14.0, 8.2, 5.8 Hz, 1H), 2.09 (dddd, *J* = 15.5, 11.9, 7.7, 5.9 Hz, 1H). ^{13}C NMR (101 MHz, MeOD) δ 163.11, 151.43, 140.90, 137.88, 130.12, 129.56, 127.23, 122.52, 116.36, 114.39, 100.06, 80.94, 49.28, 38.57, 35.94. LC/MS (ESI): 312.57 $[M+H]^+$; HRMS (TOF, ESI+) cald for $C_{17}H_{17}N_3O3$ $[M+H]^+$ 312.134, found 312.13243; Yellow oil. Yield = 18 %

*4.1.8. General procedure for synthesis of derivatives **77–79** via a nitro reduction reaction*

To a solution of nitrobenzene derivative (0.22 mmol, 1 eq) in ethyl acetate (3 mL) was added Tin (II) chloride (207 mg, 1.09 mmol) and the reaction mixture was heated at 70 °C in a sealed tube for 2h. After the solution was cooled to room temperature, the mixture was washed twice with a solution of saturated Na_2CO_3 and once with brine. The organic phase was dried over Na_2SO_4 and concentrated under vacuum. The crude product was purified by flash chromatography from DCM to DCM/MeOH 8/2 (v/v).

*4.1.8.1. 2-methyl-3-[(1S)-3-(methylamino)-1-phenylpropoxy]aniline **77**.* ^{1}H NMR (400 MHz, MeOD) δ 7.40–7.30 (m, 4H), 7.29–7.22 (m, 1H), 6.71 (bt, *J* = 8.2 Hz, 1H), 6.32 (bd, *J* = 8.0 Hz, 1H), 6.15 (bd, *J* = 8.2 Hz, 1H), 5.36 (dd, *J* = 8.2, 4.2 Hz, 1H), 3.27–3.10 (m, 2H), 2.70 (s, 3H), 2.34 (dddd, 14.0, 9.8, 8.3, 5.8 Hz), 2.22 (dddd, 13.9, 10.0, 5.7, 4.3 Hz), 2.13 (s, 3H). ^{13}C NMR (101 MHz, MeOD) δ 156.91, 147.70, 142.19, 129.79, 129.06, 127.17, 127.01, 112.67, 110.42, 105.29, 78.19, 47.74, 36.02, 33.85, 9.57. LC/MS (ESI): 271.63 $[M+H]^+$; HRMS (TOF, ESI+) cald for $C_{17}H_{22}N_2O$ $[M+H]^+$ 271.180, found 371.1805. Colorless oil. Yield = 22 %.

*4.1.8.2. 5-Chloro-2-[(1S)-3-(methylamino)-1-phenylpropoxy]aniline **78**.* ^{1}H NMR (400 MHz, MeOD) δ 7.43–7.32 (m, 4H), 7.32–7.27 (m, 1H), 6.72 (d, *J* = 2.5 Hz, 1H), 6.54 (d, *J* = 8.7 Hz, 1H), 6.41 (dd, *J* = 8.6, 2.5 Hz, 1H), 5.38 (dd, *J* = 8.6, 4.0 Hz, 1H), 3.29–3.16 (m, 2H), 2.72 (s, 3H), 2.43–2.31 (m, 1H), 2.28–2.18 (m, 1H). ^{13}C NMR (101 MHz, MeOD) δ 144.86, 141.49, 140.15, 129.95, 129.36, 127.58, 127.00, 117.87, 116.04, 115.69, 78.99, 47.67, 35.92, 33.86. LC/MS (ESI): 291.36 $[M+H]^+$; HRMS (TOF, ESI+) cald for C16H19ClN2O $[M+H]^+$ 291.126, found 291.1259; Colorless oil. Yield = 35 %.

*4.1.8.3. 2-amino-4-[(1S)-3-(methylamino)-1-phenylpropoxy]benzonitrile **79**.* ^{1}H NMR (500 MHz, MeOD) δ 7.37–7.32 (m, 4H), 7.31–7.21 (m, 1H), 7.16 (d, *J* = 8.6 Hz, 1H), 6.27 (d, *J* = 2.2 Hz, 1H), 6.24 (dd, *J* = 8.7, 2.3 Hz, 1H), 5.34 (dd, *J* = 8.2, 4.6 Hz, 1H), 2.87–2.72 (m, 2H), 2.44 (s, 3H), 2.19 (dtd, *J* = 14.0, 8.4, 5.8 Hz, 1H), 2.11–2.01 (m, 1H). ^{13}C NMR (126 MHz, MeOD) δ 163.99, 154.38, 142.14, 134.72, 129.81, 129.01, 126.97, 119.21, 107.48, 102.23, 88.75, 79.19, 48.60, 38.32, 35.55. LC/MS (ESI): 282.42 $[M+H]^+$; HRMS (TOF, ESI+) cald for C17H19N3O $[M+H]^+$ 282.160, found 282.1601. Colorless oil. Yield = 5 %.

*4.1.9. General procedure for the synthesis of amine derivatives **81–82***

To a solution of 1-[(1S)-3-chloro-1-phenylpropoxy]-4-iodobenzene **80** (200 mg, 0.54 mmol, 1eq) in dry THF (5 mL) was added sodium iodide (0.80 mmol, 1.5 eq). The mixture was heated at 70 °C for 16h. Then, the corresponding amine derivative (2.7 mmol, 5 eq) was added and the mixture was stirred under argon atmosphere at room temperature during 10–20h. After completion of the reaction, the solvent was evaporated *in vacuo*. The residue was extracted with dichloromethane, the organic layer was washed twice with water, once with brine, dried over Na2SO4, and evaporated *in vacuo*. Crude was purified by column chromatography eluting with dichloromethane-methanol (100–90:10) to give derivatives **81–82**.

*4.1.9.1. [(3S)-3-(4-iodophenoxy)-3-phenylpropyl]dimethylamine **81**.* ^{1}H NMR (400 MHz, MeOD) δ 7.43 (d, *J* = 9.0 Hz, 2H), 7.38–7.28 (m, 4H), 7.27–7.21 (m, 1H), 6.66 (d, *J* = 9.0 Hz, 2H), 5.25 (dd, *J* = 8.1, 4.8 Hz, 1H), 2.61–2.42 (m, 2H), 2.27 (s, 6H), 2.21–2.09 (m, 1H), 2.06–1.95 (m, 1H).^{13}C NMR (101 MHz, MeOD) δ 159.29, 142.47, 139.21, 129.73, 128.88, 127.13, 119.52, 83.45, 79.42, 56.76, 45.36, 37.12. LC/MS (ESI): 382.18 $[M+H]^+$; HRMS (TOF, ESI+) cald for C17H20INO $[M+H]^+$ 382.066, found 382.0662; Yellow oil. Yield = 20 %

*4.1.9.2. 1-[(3S)-3-(4-iodophenoxy)-3-phenylpropyl]pyrrolidine **82**.* ^{1}H NMR (400 MHz,MeOD) δ 7.44 (d, *J* = 9.0 Hz, 2H), 7.37–7.29 (m, 4H), 7.29–7.21 (m, 1H), 6.67 (d, *J* = 9.0 Hz, 2H), 5.26 (dd, *J* = 8.1, 4.8 Hz, 1H), 2.71 (ddd, *J* = 11.9, 10.6, 5.0 Hz, 1H), 2.65–2.60 (m, 1H), 2.62–2.54 (m, 4H), 2.20 (dddd, *J* = 13.1, 10.3, 8.0, 5.0 Hz, 1H), 2.05 (ddt, *J* = 13.6, 10.5, 5.4 Hz, 1H), 1.85–1.76 (m, 4H).^{13}C NMR (101 MHz, MeOD) δ 159.34, 142.54, 139.23, 129.72, 128.87, 127.15, 119.52, 83.40, 79.55, 55.06, 53.67, 38.46, 24.17. LC/MS (ESI): 408.04 $[M+H]^+$; HRMS (TOF, ESI+) cald for $C_{19}H_{22}$INO $[M+H]^+$ 308.082, found 408.0819; Colorless oil. Yield = 37 %.

*4.1.10. Synthesis of (3S)-3-(4-iodophenoxy)-3-phenylpropan-1-amine **83***

To a stirring suspension of potassium phthalimide (3 mmol, 1.5eq) in dry dimethylformamide (15 mL) was added the intermediate **80** (750 mg, 2 mmol). The reaction mixture was heated to 90 °C and left stirring for 4 h, until completion was observed by TLC. The reaction mixture was concentrated *in vacuo* and the resulting residue was diluted

in dichloromethane, washed twice with water, once with brine, dried over Na2SO4, and evaporated *in vacuo*. The crude residue (860 mg) obtained was then diluted in ethanol (25 mL) and hydrazine monohydrate was added (170 mg, 3 mmol) and the reaction mixture was stirred and heated to reflux for 3 h. Upon completion the reaction mixture was concentrated under reduced pressure, diluted in dichloromethane, washed twice with water, once with brine, dried over Na2SO4, and evaporated *in vacuo*. The residue was purified by flash column chromatography eluting with DCM to DCM/MeOH 90/10 (v/v) to give the pure derivative **83** as a light-yellow oil with 68 % yield. ^{1}H NMR (400 MHz,MeOD) δ 7.43 (d, J = 9.1 Hz, 2H), 7.37–7.28 (m, 4H), 7.26–7.20 (m, 1H), 6.66 (d, J = 9.1 Hz, 2H), 5.29 (dd, J = 8.3, 4.8 Hz, 1H), 2.88–2.72 (m, 2H), 2.14 (dtd, J = 14.0, 7.9, 6.0 Hz, 1H), 2.02–1.91 (m, 1H). ^{13}C NMR (101 MHz, MeOD) δ 159.31, 142.65, 139.20, 129.70, 128.79, 127.10, 119.52, 83.39, 79.43, 42.33, 39.10. LC/MS (ESI): 354.29 $[M+H]^+$; HRMS (TOF, ESI+) cald for $C_{15}H_{16}INO$ $[M+H]^+$ 354.034, found 354.0349.

4.1.11. Synthesis of N-[(3S)-3-(4-iodophenoxy)-3-phenylpropyl]guanidine **84**

The commercial 1*H*-pyrazole-1-carboxamidine hydrochloride (96 mg, 6.6 mmol, 1.1 eq) was suspended in dry dimethylformamide (10 mL) under argon and diisopropylethylamine was added (115 μL, 6.6 mmol, 1.1 eq). Then, a solution of compound **83** (212 mg, 6.1 mmol) in DMF (2 mL) was added dropwise. The mixture was stirred at room temperature under nitrogen for 16 h and the solvent was removed *in vacuo*. The remaining viscous yellow oil was treated with ~1 mL saturated $NaHCO_3$ solution, immediately forming a white crystalline precipitate, which was filtered off, washed with $NaHCO_3$ solution, water and diethyl ether, and dried *in vacuo* yielding the pure product **84** as an off-white crystalline solid. Yield = 80 %. ^{1}H NMR (400 MHz, MeOD) δ 7.45 (d, J = 8.9 Hz, 2H), 7.40–7.31 (m, 4H), 7.30–7.23 (m, 1H), 6.69 (d, J = 8.9 Hz, 2H), 5.30 (dd, J = 8.9, 4.2 Hz, 1H), 3.44–3.34 (m, 2H), 2.28–2.16 (m, 1H), 2.09 (dtd, J = 11.6, 7.3, 4.2 Hz, 1H). ^{13}C NMR (101 MHz, MeOD) δ 159.12, 158.92, 142.02, 139.26, 129.87, 129.07, 127.08, 119.56, 83.70, 78.71, 39.37, 38.78. LC/MS (ESI): 396.29 $[M+H]^+$; HRMS (TOF, ESI+) cald for C16H18IN3O $[M+H]^+$ 396.056, found 396.0567.

4.2. Molecular modeling

4.2.1. Binding site preparation

Two structures of the RNA helicase domain of the CV-B3 2C protein complexed with (*S*)-fluoxetine are available in the RCSB PDB [35] (PDB. ID 6s3a and 6t3w) [13]. In these two structures, the poses of the fluoxetine compound are highly superimposed, except for the N-methylamine group which is exposed to the solvent. As the structure with PDB.ID 6s3a has the best crystallographic resolution (1.52 Å vs 1.82 Å for PDB.ID 6t3w), we choose this structure as the target structure to conduct the docking experiments.

The receptor was prepared using the Protein Preparation Wizard workflow [36] from the Schrödinger Molecular Modelling Suite 2022–03. Water molecules were first removed and missing side chains of residues were fulfilled. Then, hydrogen atoms were added to the receptor according to a global target pH value of 7.4, and the hydrogen network was automatically optimised. Finally, the receptor was minimised (OLPS2004 force field) [37] with a convergence criterion of RMSD on heavy atoms of 0.3 Å (other parameters were fixed to their default values).

4.2.2. Design of a virtual library

A total of 140 fluoxetine analogues were designed and stored as a 2D SDF structure file for virtual screening experiment, in addition with the 2D structures of (*R*)- and (*S*)-fluoxetine. All these compounds were prepared using the LigPrep package [38] of the Schrödinger Molecular Modelling Suite 2022–03 with default parameters, including the generation of tautomeric and ionization states and stereoisomers, resulting in 163 3D structures of compounds for the docking.

4.2.3. Virtual screening

Docking experiments were carried out using the Glide software [39–41] from the Schrödinger Suite. The docking grid was centered and sized on the crystalized fluoxetine. Docking calculations were performed with extra precision. Ligand flexibility was considered and the option of sampling of ring conformation was activated. Only one pose was generated by compound.

4.3. Biology

4.3.1. Cells and viruses

HeLa CCL-2 cells and Rhabdomyosarcoma (RD) cells were provided by ATCC. They were cultured in Minimum Essential Medium (MEM, Gibco) supplemented with 7.5 % fetal bovine serum (FBS; Gibco), 1 % L-Glutamine (Gibco), 1 % non-essential amino acid (Gibco) and 1 % Penicillin - Streptomycin (10 000 U/ml; Gibco). Both cell lines were grown at 37 °C in 5 % CO_2.

Enterovirus A71 (EV-A71, clinical strain Laos2011 HFMD18TS) was provided through the European Virus Archive (**Ref-SKU**: 001v-EVA1553). Coxsackievirus B3 (CV–B3, strain Nancy) was provided by ATCC. Enterovirus D68 (EV-D68 (strain 316.183.054) was provided by the French National Reference Center for Enteroviruses and Parechoviruses (Clermont-Ferrand University Hospital, France).

4.3.2. Antiviral assay and EC_{50} determination

One day prior to infection, 30 000 RD cells, or 15 000 HeLa CCL-2 cells, per well were seeded in 100 μL assay medium containing 2.5 % FBS in 96-well culture plates (Falcon® 96-well clear microplate, Corning). After 24 h, antiviral compounds were added with seven ½ dilutions. Each experiment was performed in triplicate. Then, 25 μL/well of a virus mix diluted in the medium was added to the wells. Prior to the assay, it was verified that viruses in the cell culture supernatants were harvested during the logarithmic growth phase of viral replication at 48h or 72h post infection measured by RT-qPCR. Thus, 96-well plates infected with EV-A71 were incubated at 37 °C for 48h, plates infected with CV-B3 were incubated at 37 °C for 72h and plates infected with EV-D68 were incubated at 33 °C for 72h. Vapendavir (MedChemExpress), S-fluoxetine and A-967079 (MedChemExpress) were used as positive controls and added to each plate in assays against EV-A71, CV-B3 and EV-D68, respectively. For EV-A71 assays, on each plate, Vapendavir (Medchemexpress) was used as a positive control. For CV-B3 assays, (*S*)-fluoxetine was used as a positive control. For EV-D68 assays, A-967079 (MedChemExpress) was used as a positive control.[32] 3 compounds were tested per 96-well plate, using a virus control (VC) in triplicate 48h or 72h post-infection, the supernatant was harvested, and RNA was quantified as described above. Antiviral efficacy was evaluated in a range of compound concentrations from 16 μM to 0.25 μM. In each well, the percentage of viral inhibition VI was calculated as follows:

$$VI = 100 * \frac{(mean\ RNA\ quantity\ VC - RNA\ quantity\ in\ the\ well)}{mean\ RNA\ quantity\ VC}$$

The 50 % effective concentrations (EC_{50}, compound concentration required to inhibit viral RNA replication by 50 %) were determined by logarithmic interpolation after performing a nonlinear regression (log (inhibitor) vs. response–variable slope (four parameters)), using GraphPad Prism 9 software (GraphPad software). For cytopathic effect (CPE) assay, 96-well plates of RD cells infected with EV-D68 were prepared as described above. After three days of incubation at 33 °C, the supernatant was removed and CellTiterBlue® (Promega) reagent was added to the cells following the manufacturer's recommendations. After 2 h of incubation at 37 °C, fluorescence was measured using an Infinite 200 Pro plate reader (Tecan Life Sciences). The EC_{50} value was determined as described above, using GraphPad Prism 9 software.

4.3.3. Plaque assay

One day prior infection, ~450 000 RD cells per well were in 1.5 mL MEM containing 2.5 % FBS in 12-well culture plates (Falcon®, Corning®). After overnight incubation at 37 °C, the cell culture medium was removed, and the cell monolayer was washed with 1 mL of Hanks' Balanced Salt Solution (HBSS, Gibco). Cells were then infected with EV-D68 virus diluted with culture medium containing 0 % FBS, and incubated at 33 °C for 1 h. Unbound virus particles were removed by HBSS wash. Overlay containing the serially diluted compound, MEM with 2.5 % FBS and 1.2 % Avicel (Sigma-Aldrich) was added to the cells with 1.5 mL per well. Plates were incubated at 33 °C with 5 % CO_2 for 3 days. After removing the overlay and washing with HBSS, cells were fixed with 4 % formaldehyde in HBSS, and stained with 1 % crystal violet in HBSS.

4.3.4. Cytotoxicity and CC_{50} determination

Cytotoxicity of the compounds was assessed using the CellTiterBlue® cell viability assay (Promega), in a range of compound concentration from 100 µM to 1 µM. 96-well culture plates were prepared in a similar way to the antiviral assay, but with the addition of 25 µl of culture medium instead of the virus mixture. After 72 h incubation, fluorescence was measured using an Infinite 200 Pro plate reader (Tecan Life Sciences). Like the EC_{50}, the 50 % cytotoxic concentration (CC_{50}, compound concentration inducing the death of 50 % of cells) was determined by logarithmic interpolation after performing a nonlinear regression (log(inhibitor) vs. response–variable slope (four parameters)), using GraphPad Prism 9 software (GraphPad software).

4.3.5. Viral RNA extraction and quantification

Viral RNA was extracted from 100 µL of cell culture supernatant using a QIAamp Viral RNA kit on the automated QIAcube (Qiagen), according to the manufacturer's instructions. Relative quantification of viral RNA was performed using the GoTaq® 1-Step RT-qPCR System kit (Promega). The mixture contained 5 µL of 2x Master Mix, 0.25 µL of each primer (250 nM), 0.07 µL of probe (75 nM), 0.2 µL of GoScript RT Mix and 3.8 µL of extracted nucleic acids. For EV-A71, EV-A71F: 5′-AGATACCCACCCCCCTTACAA-3′, EV-A71R: 5′-CACGTACGGGTGTTGCAACT-3′, and EV-A71P FAM-5′-CTCAACCCGGCGCC-3′-MGB were used as primers and probe. For CV-B3, a pan Enterovirus system already reported was used [42]. For EV-D68, an EV-D68 specific system already reported was used [43]. Assays were performed using the QuantStudio 12 K Flex real-time PCR machine (Life technologies). Reaction mixtures were exposed at 50 °C for 15 min, then 95 °C for 2 min, followed by 40 cycles of 95 °C for 3 s, then 60 °C for 30 s. Data collection took place during the 60 °C step. *In vitro* transcripts were used to calculate the amount of viral RNA from standard curves.

4.3.6. Cloning and construct design

Several constructs of the CV-B3 2C and EV-A71 2C proteins were generated for specific needs. For binding assays with CV-B3 2C, the DNA fragment coding for CV- B3 Δ36-2C (amino acids 37 to 329) was cloned downstream of a cleavable thioredoxin-hexahistidine tag (PMID: 31305993). For binding assays with EV-A71 2C, the coding sequence of EV-A71 Δ116-2C (amino acids 117 to 329) was cloned into the expression vector pmCox 20A as previously described [44]. For protein crystallization and structural determination, the coding sequence of CV-B3 Δ116-2C (amino acids 117 to 329) was cloned into the expression vector pmCox 20A. For ATPase assays, the coding sequences of an hexamerization domain and CV-B3 Δ116-2C was previously fused and cloned to generate the hexΔ116-2C constructs [13].

4.3.7. Protein expression and purification

The three recombinant proteins were produced in *Escherichia coli* T7 Express (New England biolabs). Cells were grown in TB (Terrific Broth) medium supplemented with glycerol and containing ampicillin (100 µg/ml) or kanamycin (100 µg/ml) and chloramphenicol (34 µg/ml) at 37 °C. Expression was induced overnight at 17 °C with 0.5 mM isopropyl-thiogalactopyranoside (IPTG). The cells were harvested by centrifugation and resuspended in lysis buffer (50 mM tris, 300 mM NaCl, 10 mM imidazole, 5 % glycerol, and 0.1 % Triton X-100) complemented with lysozyme (0.25 mg/ml), deoxyribonuclease (DNase; 10 µg/ml), and 1 mM phenylmethylsulfonyl fluoride (PMSF). The bacterial samples were sonicated and centrifuged at 12,000g for 30 min at 4 °C. Soluble CV-B3 Δ36-2C, CV-B3 and EV-A71 Δ116-2C, and CV-B3 hexΔ116-2C, were purified from the supernatant by immobilized metal affinity chromatography (IMAC) on a HisTrap column (GE Healthcare) and eluted with a buffer consisting of 50 mM tris, 300 mM NaCl, and 500 mM imidazole (pH 8). The eluted Δ36-2C and Δ116-2C proteins were subjected to dialysis in 50 mM tris (pH 8), 300 mM NaCl, 10 mM imidazole, and 1 mM DTT (dithiothreitol), followed by an overnight cleavage by Tobacco Etch Virus (TEV) protease (molar ratio, 1/20), followed by a second IMAC to remove the tag and uncleaved proteins. The recombinant proteins were lastly purified by SEC on a HiLoad 16/60 Superdex 75 column (GE Healthcare) in 10 mM HEPES (pH 7.5) and 300 mM NaCl. The protein-containing fractions were pooled, concentrated, and stored at −80 °C. For ATPase assays, the hexΔ116-2C TEV protease tag was not cleaved. After the first IMAC, the eluted protein was purified by SEC on a HiLoad 16/60 Superdex 200 column (GE Healthcare) in 10 mM HEPES (pH 7.5), 150 mM NaCl, and 10 mM $MgCl_2$. Protein fractions corresponding to the SEC peak at the hexameric molecular weight were pooled, concentrated, and stored at −20 °C in 20-µl aliquots containing 50 % glycerol, with a final concentration of ~4 mg/ml.

4.3.8. Binding of compounds to 2C protein

The binding of compounds on CV-B3 Δ36-2C and EV-A71 Δ116-2C proteins was monitored by the fluorescence-based thermal shift assay (TSA) using a Bio-Rad CFX Connect (Bio-Rad), as previously described [19].

4.3.9. ATPase assay

The release of inorganic phosphate during 2C-mediated ATPase hydrolysis was measured using the Malachite Green Phosphate Assay Kit (Sigma-Aldrich). ATP was purchased from Cytiva (ref 27-2056-01). Each 25-µl reaction comprised 500 nM of CV-B3 hexΔ116-2C protein and 1 mM ATP in reaction buffer (10 mM HEPES (pH 7.5), 150 mM NaCl, and 10 mM $MgCl_2$). The reaction buffer and recombinant protein were thawed immediately before use. For testing the inhibitory effect of 2C-targeting compounds, the final DMSO concentration in each reaction was 1 %. The compound-enzyme mixture was incubated for 15 min at 4 °C before adding ATP. Reactions were performed for 15 min at 37 °C. To stop the reaction, 20 µl were transferred to a 96-well reading plate at 4 °C, and mixed with 10 µl of 10 mM EDTA. Samples were then diluted with water to give a final ATP concentration of 0.25 mM before adding the working reagent, as per the manufacturer's instructions. The plates were incubated for 30 min at room temperature, and absorbance was measured using a microplate reader at OD_{620nm}. To determine the phosphate concentration in each sample, the OD_{620nm} values were plotted against a standard curve using GraphPad Prism 9 software (GraphPad software).

4.4. Crystallography

4.4.1. Co-crystallization of CV-B3 Δ116-2C protein and compound **53**

Structure Screens 1 and 2 and Stura Footprint Screen (Molecular Dimensions Ltd.) were used for initial screening. Trials were assessed in SWISSCI 3 Lens Crystallization Plates with three wells per reservoir using 400-, 300-, and 200-nl drops. The drops contained increasing volumes (100, 200, and 300 nl) of protein solution at a concentration of 10 mg/ml in complex with 2 mM of compound **53** (from 100 mM stock in 100 % DMSO) and 100 nl of mother liquor. Crystals were observed in 0.2 M imidazole malate (pH 7.0) and polyethylene glycol (PEG) 4K

10–20 %. They were soaked in 20 % (v/v) PEG 200 added to the mother liquor and cooled in liquid nitrogen. X-ray diffraction data were collected at the European Synchrotron Radiation Facility, at SOLEIL synchrotron (Proxima 2). The space group was assigned to $P2_12_12_1$ with one protein and one **53** compound per asymmetric unit (PDB code 9RQK). We used Pipedream [45], a tool specifically designed for linking data processing with AutoPROC, rigid-body replacement with Phaser, and structure refinement with autoBUSTER. Using this automated pipeline, images were processed and scaled using XDS [46] and SCALA. The structure of CV-B3 Δ116-2C protein (PDB ID 6S3A) was used as template model in the limited molecular replacement procedure and the structure was refined to a resolution of 1.7 Å. Iterative cycles of model building were done with the program COOT. Compounds restraints were generated with grade [47] and Mogul [48] using RM1 semi-empirical QM methods.

Funding

This work was supported by grants from the French National Research Agency (ANR-23-CE18-0023-01, Project Fluox2C), the French Infrastructure for Integrated Structural Biology (FRISBI) ANR-10-INSB-05-01 with the use of Marseille integrative structural biology facility (PBSIM) at the AFMB lab.

CRediT authorship contribution statement

Safeh Khemiri: Investigation, Methodology, Writing – original draft, Investigation. **Marine O. Faucher:** Investigation, Methodology, Writing – original draft. **Stephane Bourg:** Investigation, Methodology. **Sarah Attoumani-Madi:** Investigation. **Carole Yaacoub:** Investigation. **Franck Touret:** Writing – review & editing. **Marc Farag:** Investigation, Methodology. **Mattéo Fermiana Vitorino:** Investigation. **Pascal Bonnet:** Project administration, Resources, Writing – review & editing. **Patrice Vanelle:** Resources, Writing – review & editing. **Samia Aci-Seche:** Funding acquisition, Investigation, Methodology, Project administration, Supervision, Writing – original draft, Writing – review & editing. **Bruno Coutard:** Conceptualization, Funding acquisition, Investigation, Methodology, Project administration, Supervision, Writing – original draft, Writing – review & editing. **Karine Barral:** Conceptualization, Funding acquisition, Investigation, Methodology, Project administration, Supervision, Writing – original draft, Writing – review & editing.

Declaration of competing interest

The authors declare that they have no known competing financial interests or personal relationships that could have appeared to influence the work reported in this paper.

Acknowledgements

We wish to thank Justine Le Meur and Chrisnad Mindzie Mi Ovono Avome for their technical assistance, as well the CNR for Enterovirus and Paraechoviruses (laboratoire de virologie du CHU de Clermont-Ferrand) for kindly providing the EVD-68 strain. The authors acknowledge the European Synchrotron Radiation Facility (ESRF) as well as the SOLEIL synchrotron (Proxima 1 and Proxima 2 beamlines) for provision of synchrotron radiation facilities, the Chiropole plateform (UAR1739, Marseille) and the Marseille Screening Center MaSC platform (IBiSA and Platform Aix Marseille labels). For their financial support of ICOA, UMR 7311, University of Orléans, CNRS, we also wish to thank the projects CHemBio (FEDER-FSE 2014-2020-EX003677), Valbiocosm (FEDER-FSE 2014-2020-EX003202), Techsab (FEDER-FSE 2014-2020-EX011313), QUALICHIM (APR-IA-PF 2021-00149467), Project ESTIM-ICOA (CPER/FEDER-FSE+ 2021-2027-00022860), the RTR Motivhealth (2019–00131403), the Labex programs SYNORG (ANR-11-LABX-0029) and IRON (ANR-11-LABX-0018-01).

List of abbreviations

CC_{50}, inhibitor concentration inducing 50 % cell death; CV, coxsackievirus; DCM, dichloromethane; DIAD, diisopropyl azodicarboxylate; DIEA, *N,N*-diisopropylethylamine; DMF, *N,N*-dimethylformamide; DMSO, dimethylsulfoxide; EC_{50}, efficacy concentration required to inhibit 50 % of the virus on infected cells; EDCI, 1-ethyl-3-(3-dimethylaminopropyl)carbodiimide; ee, enantiomeric excess; EV, enterovirus; FA, formic acid; IC_{50}, cytotoxic concentration required to inhibit 50 % of enzyme activity; NMR, nuclear magnetic resonance; PDB, protein data bank; RD, PPh_3, triphenylphosphine; Rhabdomyosarcoma; rt, room temperature; RT, retention time; SAR, Structure-activity relationship; SD, standard deviation; LC/MS, liquid chromatography/mass spectroscopy; SI, selectivity index; SNAr, nucleophilic aromatic substitution; SSRI, selective serotonin reuptake inhibitor; TFA, trifluoroacetic acid; THF, tetrahydrofuran; TLC, thin layer chromatography; T_m, melting temperature TSA, Thermal-Shift Assay; VS, virtual screening.

Appendix A. Supplementary data

Supplementary data to this article can be found online at https://doi.org/10.1016/j.ejmech.2026.118621.

Data availability

Data will be made available on request.

References

[1] L. Brouwer, G. Moreni, K.C. Wolthers, D. Pajkrt, World-Wide prevalence and genotype distribution of enteroviruses, Viruses 13 (2021) 434, https://doi.org/10.3390/v13030434.
[2] P. Simmonds, A.E. Gorbalenya, H. Harvala, T. Hovi, N.J. Knowles, A.M. Lindberg, M.S. Oberste, A.C. Palmenberg, G. Reuter, T. Skern, C. Tapparel, K.C. Wolthers, P. C.Y. Woo, R. Zell, Recommendations for the nomenclature of enteroviruses and rhinoviruses, Arch. Virol. 165 (3) (2020) 793–797, https://doi.org/10.1007/s00705-019-04520-6.
[3] N.M. Chapman, K.S. Kim, Persistent coxsackievirus infection: enterovirus persistence in chronic myocarditis and dilated cardiomyopathy, Curr. Top. Microbiol. Immunol. 323 (2008) 275–292, https://doi.org/10.1007/978-3-540-75546-3_13.
[4] C. Tapparel, F. Siegrist, T.J. Petty, L. Kaiser, Picornavirus and enterovirus diversity with associated human diseases, Infect. Genet. Evol. 14 (2013) 282–293, https://doi.org/10.1016/j.meegid.2012.10.016.
[5] J. Puenpa, N. Wanlapakorn, S. Vongpunsawad, Y. Poovorawan, The history of enterovirus A71 outbreaks and molecular epidemiology in the Asia-Pacific Region, J. Biomed. Sci. 26 (1) (2019) 75, https://doi.org/10.1186/s12929-019-0573-2.
[6] K. Messacar, T.L. Schreiner, J.A. Maloney, A. Wallace, J. Ludke, M.S. Oberste, W. A. Nix, C.C. Robinson, M.P. Glodé, M.J. Abzug, S.R. Dominguez, A cluster of acute flaccid paralysis and cranial nerve dysfunction temporally associated with an outbreak of enterovirus D68 in children in Colorado, USA, Lancet 385 (9978) (2015) 1662–1671, https://doi.org/10.1016/S0140-6736(14)62457-0.
[7] C.Y. Kim, B. Piamonte, R. Alle, K.T. Thakur, Threat of resurgence or hope for global eradication of poliovirus? Curr. Opin. Neurol. 36 (3) (2023) 229–237, https://doi.org/10.1097/WCO.0000000000001156.
[8] P. Zhu, W. Ji, D. Li, Z. Li, Y. Chen, B. Dai, S. Han, S. Chen, Y. Jin, G. Duan, Current status of hand-foot-and-mouth disease, J. Biomed. Sci. 30 (1) (2023) 15, https://doi.org/10.1186/s12929-023-00908-4.
[9] P.L. Rodríguez, L. Carrasco, Poliovirus protein 2C has ATPase and GTPase activities, J. Biol. Chem. 268 (11) (1993) 8105–8110, https://doi.org/10.1016/S0021-9258(18)53068-4.
[10] H. Xia, P. Wang, G.C. Wang, J. Yang, X. Sun, W. Wu, Y. Qiu, T. Shu, X. Zhao, L. Yin, C.F. Qin, Y. Hu, X. Zhou, Human Enterovirus nonstructural protein 2CATPase functions as both an RNA helicase and ATP-Independent RNA chaperone, PLoS Pathog. 11 (7) (2015) e1005067, https://doi.org/10.1371/journal.ppat.1005067.
[11] S.-H. Wang, K. Wang, K. Zhao, S.-C. Hua, J. Du, The structure, function, and mechanisms of action of enterovirus non-structural protein 2C, Front. Microbiol. 11 (2020) 615965, https://doi.org/10.3389/fmicb.2020.615965.
[12] P. Chen, Z. Li, S. Cui, Picornaviral 2C Proteins: a Unique Atpase Family Critical in Virus Replication, the Enzymes, vol. 49, 2021, pp. 235–264, https://doi.org/10.1016/bs.enz.2021.06.008.
[13] D.L. Hurdiss, P. El Kazzi, L. Bauer, N. Papageorgiou, F.P. Ferron, T. Donselaar, A.L. W. van Vliet, T.M. Shamorkina, J. Snijder, B. Canard, E. Decroly, A. Brancale,

T. Zeev-Ben-Mordehai, F. Förster, F.J.M. van Kuppeveld, B. Coutard, Fluoxetine targets an allosteric site in the enterovirus 2C AAA+ ATPase and stabilizes a ring-shaped hexameric complex, Sci. Adv. 8 (2022), https://doi.org/10.1126/sciadv.abj7615.
[14] P. El Kazzi, C. Yaacoub, Z. Fajloun, P. Vanelle, E. Decoly, B. Coutard, K. Barral, 2C protein of Enterovirus: key protein of viral replication and antiviral target, Virologie 27 (3) (2023) 35–49, https://doi.org/10.1684/vir.2023.1002.
[15] J. Zuo, K.K. Quinn, S. Kye, P. Cooper, R. Damoiseaux, P. Krogstad, Fluoxetine is a potent inhibitor of coxsackievirus replication, Antimicrob. Agents Chemother. 56 (9) (2012) 4838–4844, https://doi.org/10.1128/AAC.00983-12.
[16] R. Ulferts, L. van der Linden, H.J. Thibaut, K.H. Lanke, P. Leyssen, B. Coutard, A. M. De Palma, B. Canard, J. Neyts, F.J. van Kuppeveld, Selective serotonin reuptake inhibitor fluoxetine inhibits replication of human enteroviruses B and D by targeting viral protein 2C, Antimicrob. Agents Chemother. 57 (4) (2013) 1952–1956, https://doi.org/10.1128/AAC.02084-12.
[17] J. Zuo, S. Kye, K.K. Quinn, P. Cooper, R. Damoiseaux, P. Krogstad, Discovery of structurally diverse small-molecule compounds with broad antiviral activity against enteroviruses, Antimicrob. Agents Chemother. 60 (3) (2015) 1615–1626, https://doi.org/10.1128/AAC.02646-15.
[18] R. Ulferts, M. de Boer, L. van der Linden, L. Bauer, H.R. Lyoo, M.J. Maté, J. Lichière, B. Canard, D. Lelieveld, W. Omta, D. Egan, B. Coutard, F.J. van Kuppeveld, Screening of a library of FDA- approved drugs identifies several enterovirus replicaton inhibitors that target viral protein 2C, Antimicrob. Agents Chemother. 60 (5) (2016) 2627–2638, https://doi.org/10.1128/AAC.02182-15.
[19] L. Bauer, R. Manganaro, J.R.P.M. Strating, P. El Kazzi, M. Lorenzo Lopez, R. Ulferts, C. van Hoey, M.J. Maté, T. Langer, B. Coutard, A. Brancale, F.J.M. van Kuppeveld, Fluoxetine inhibits enterovirus replication by targeting the viral 2C protein in a stereospecific manner, ACS Infect. Dis. 5 (9) (2019) 1609–1623, https://doi.org/10.1021/acsinfecdis.9b00179.
[20] A.M. Hixon, P. Clarke, K.L. Tyler, Evaluating treatment efficacy in a mouse model of Enterovirus D68–Associated paralytic myelitis, J. Infect. Dis. 216 (10) (2017) 1245–1253, https://doi.org/10.1093/infdis/jix468.
[21] J. Gofshteyn, A.M. Cárdenas, D. Bearden, Treatment of chronic Enterovirus encephalitis with fluoxetine in a patient with X-Linked Agammaglobulinemia, Pediatr. Neurol. 64 (2016) 94–98, https://doi.org/10.1016/j.pediatrneurol.2016.06.014.
[22] L. Yu, Y. Zhang, W. Li, J. Mao, Y. Li, H. Wang, C. Li, L. Yang, W. He, Y. Jia, W. Tang, L. Zhou, Z. Zhang, Y. Jia, X. Tang, X. Zhao, Y. An, Fluoxetine successfully treats intracranial enterovirus E18 infection in a patient with CD79a deficiency arising from segmental uniparental disomy of chromosome 19, J. Clin. Immunol. 44 (6) (2024) 137, https://doi.org/10.1007/s10875-024-01740-7.
[23] R. Manganaro, B. Zonsics, L. Bauer, M. Lorenzo Lopez, T. Donselaar, M. Zwaagstra, F. Saporito, S. Ferla, J.R.P.M. Strating, B. Coutard, D.L. Hurdiss, F.J.M. van Kuppeveld, A. Brancale, Synthesis and antiviral effect of novel fluoxetine analogues as enterovirus 2C inhibitors, Antiviral Res 178 (2020) 104781, https://doi.org/10.1016/j.antiviral.2020.104781.
[24] H. Finkelstein, Darstellung organischer Jodide aus den entsprechenden Bromiden und Chloriden, Ber. Dtsch. Chem. Ges. 43 (2) (1910) 1528–1532, https://doi.org/10.1002/cber.19100430257.
[25] J.-Y. Park, S.W. Kim, J.-K. Lee, W.B. Im, B.K. Jin, S.-H. Yoon, Simplified heterocyclic analogues of fluoxetine inhibit inducible nitric oxide production in lipopolysaccharide-induced BV2 cells, Biol. Pharm. Bull. 34 (4) (2011) 538–544, https://doi.org/10.1248/bpb.34.538.
[26] J.R. Cashmana, T. Voelkera, R. Johnson, A. Janowsky, Stereoselective inhibition of serotonin re-uptake and phosphodiesterase by dual inhibitors as potential agents for depression, Bioorg. Med. Chem. 17 (2009) 337–343, https://doi.org/10.1016/j.bmc.2008.10.065.
[27] L.H. Ling, B.H. Hoff, T. Anthonsen, Chemoenzymatic synthesis of the non-tricyclic antidepressants Fluoxetine, Tomoxetine and Nisoxetine, journal of the chemical society, Perkin Transactions 1 (11) (2000) 1767–1769, https://doi.org/10.1039/B000846J.
[28] F.D. Bellamy, K. Ou, Selective reduction of aromatic nitro-compounds with stannous chloride in non-acidic and non-aqueous medium, Tetrahedron Lett. 25 (1984) 839–842, https://doi.org/10.1016/S0040-4039(01)80041-1.
[29] N. Abbassi, E. Rakib, A. Hannioui, M. Alaoui, M. Benchidmi, E. Essassi, D. Geffken, Alkylation and reduction of N-Alkyl-4-nitroindazoles with anhydrous SnCl2 in ethanol: synthesis of novel 7-Ethoxy-N-alkylindazole derivatives, Heterocycles 83 (2011) 891–900, https://doi.org/10.1002/chin.201133102.
[30] H. Roux, F. Touret, A. Coluccia, P. Scio, H.S. Bouzidi, C. di Giorgio, F. Gattacceca, O. Khoumeri, R. Silvestri, P. Vanelle, M. Roche, Design and synthesis of novel thioether analogs as promising antiviral agents: in vitro activity against enteroviruses of interest, Eur. J. Med. Chem. 288 (2025) 117395, https://doi.org/10.1016/j.ejmech.2025.117395.
[31] A. Tijsma, D. Franco, S. Tucker, R. Hilgenfeld, M. Froeyen, P. Leyssen, J. Neyts, The capsid binder vapendavir and the novel protease inhibitor SG85 inhibit enterovirus 71 replication, Antimicrob. Agents Chemother. 58 (11) (2014) 6990–6992, https://doi.org/10.1128/AAC.03328-14.
[32] H. Tan, B. Pollard, K. Li, J. Wang, Discovery of A-967079 as an enterovirus D68 antiviral by targeting the viral 2C protein, Acs Infectious Deseases 10 (12) (2024) 4327–4336, https://doi.org/10.1021/acsinfecdis.4c00678.
[33] M.S. Bernatowic, Y. Wu, G.R. Matsueda, 1H-Pyrazole-1-carboxamidine hydrochloride: an attractive reagent for guanylation of amines and its application to peptide synthesis, J. Org. Chem. 57 (8) (1992) 2497–2502, https://doi.org/10.1021/jo00034a059.
[34] H. Lin, Q. Li, Q. Li, J. Zhu, K. Gu, X. Jiang, Q. Hu, F. Feng, W. Qu, Y. Chen, H. Sun, Small molecule KDM4s inhibitors as anti-cancer agents, J. Enzym. Inhib. Med. Chem. 33 (1) (2018) 777–793, https://doi.org/10.1080/14756366.2018.1455676.
[35] H.M. Berman, J. Westbrook, Z. Feng, G. Gilliland, T.N. Bhat, H. Weissig, I. N. Shindyalov, P.E. Bourne, The protein data bank, Nucleic Acids Res. 28 (1) (2000) 235–242, https://doi.org/10.1093/nar/28.1.235.
[36] G.M. Sastry, M. Adzhigirey, T. Day, R. Annabhimoju, W. Sherman, Protein and ligand preparation: parameters, protocols, and influence on virtual screening enrichments, J. Comput. Aided Mol. Des. 27 (3) (2013) 221–234, https://doi.org/10.1007/s10822-013-9644-8.
[37] C. Lu, C. Wu, D. Ghoreishi, W. Chen, L. Wang, W. Damm, G.A. Ross, M.K. Dahlgren, E. Russell, C.D. Von Bargen, R. Abel, R.A. Friesner, E.D. Harder, OPLS4: improving force field accuracy on challenging regimes of chemical space, J. Chem. Theor. Comput. 17 (7) (2021) 4291–4300, https://doi.org/10.1021/acs.jctc.1c00302.
[38] Schrödinger Release 2022-03, LigPrep, Schrödinger, LLC, New York, NY, 2022.
[39] R.A. Friesner, R.B. Murphy, M.P. Repasky, L.L. Frye, J.R. Greenwood, T.A. Halgren, P.C. Sanschagrin, D.T. Mainz, Extra precision glide: docking and scoring incorporating a model of hydrophobic enclosure for protein-ligand complexes, J. Med. Chem. 49 (21) (2006) 6177–6196, https://doi.org/10.1021/jm051256o.
[40] T.A. Halgren, R.B. Murphy, R.A. Friesner, H.S. Beard, L.L. Frye, W.T. Pollard, J. L. Banks, Glide: a new approach for rapid, accurate docking and scoring. 2. Enrichment factors in database screening, J. Med. Chem. 47 (7) (2004) 1750–1759, https://doi.org/10.1021/jm030644s.
[41] R.A. Friesner, J.L. Banks, R.B. Murphy, T.A. Halgren, J.J. Klicic, D.T. Mainz, M. P. Repasky, E.H. Knoll, M. Shelley, J.K. Perry, D.E. Shaw, P. Francis, P.S. Shenkin, Glide : a new approach for rapid, accurate docking and scoring. 1. Method and assessment of docking accuracy, J. Med. Chem. 47 (7) (2004) 1739–1749, https://doi.org/10.1021/jm0306430.
[42] T. Watkins-Riedel, M. Woegerbauer, D. Hollemann, P. Hufnagl, Rapid diagnosis of enterovirus infections by real-time PCR on the LightCycler using the TaqMan format, Diagn. Microbiol. Infect. Dis. 42 (2) (2002) 99–105, https://doi.org/10.1016/s0732-8893(01)00330-3.
[43] R. Poelman, E.H. Schölvinck, R. Borger, H.G. Niesters, C. van Leer-Buter, The emergence of enterovirus D68 in a Dutch university medical center and the necessity for routinely screening for respiratory viruses, J. Clin. Virol. 62 (2015) 1–5, https://doi.org/10.1016/j.jcv.2014.11.011.
[44] V. Lantez, K. Dalle, R. Charrel, C. Baronti, B. Canard, B. Coutard, Comparative production analysis of three phlebovirus nucleoproteins under denaturing or non-denaturing conditions for crystallographic studies, PLoS Neglected Trop. Dis. 5 (1) (2011) e936, https://doi.org/10.1371/journal.pntd.0000936.
[45] A. Sharff, P. Keller, C. Vonrhein, O. Smart, T. Womack, C. Flensburg, C. Paciorek, G. Bricogne, Pipedream, Version 0.1.4, Global Phasing Ltd, Cambridge, United Kingdom, 2011.
[46] W. Kabsch, Xds, Acta Crystallogr D Biol Crystallogr 66 (Pt 2) (2010) 125–132, https://doi.org/10.1107/S0907444909047337. DOI: S0907444909047337 [pii].
[47] O.S. Smart, T.O. Womack, A. Sharff, C. Flensburg, P. Keller, W. Paciorek, C. Vonrhein, G. Bricogne, Grade, Version 1.1.1, Global Phasing Ltd, Cambridge, United Kingdom, 2011.
[48] I.J. Bruno, J.C. Cole, M. Kessler, J. Luo, W.D. Motherwell, L.H. Purkis, B.R. Smith, R. Taylor, R.I. Cooper, S.E. Harris, Retrieval of crystallographically-derived molecular geometry information, J. Chem. Inf. Comput. Sci. 44 (6) (2004) 2133–2144, https://doi.org/10.1021/ci049780b.